AN ABSTRACT OF THE THESIS OF

Douglas W. Prihar for the degree of Master of Science in Geology presented on February 10, 1987

Title: Geology and Mineralization of the Seaman Gulch Area, East Shasta Mining District, Shasta County, California

Redacted for privacy

Abstract approved: Cyrus W. Field

The Seaman Gulch area is located approximately 20 miles east of Redding, California and is part of the eastern Klamath lithotectonic belt.

Rock units of the area are chiefly mafic and silicic volcanics of island arc affinity and shale that are Permian to Triassic in age. Volcanic rocks of Tertiary and Quaternary age unconformably overlie the pre-Tertiary rocks. All pre-Tertiary rocks have been altered by hydrothermal and(or) metamorphic processes.

Stratabound epigenetic mineralization is hosted by metadacitic pyroclastics of the Bully Hill Rhyolite. The hypogene sulfide minerals present are pyrite, sphalerite, chalcopyrite, tetrahedrite-tennantite and galena. Minor amounts of supergene chalcocite are found. These sulfides occur as disseminations, stringer veinlets, massive pods and an irregular network around pyroclastic fragments. Controls that localized the occurrences of sulfides are intrusive rock-country rock contacts, permeability and

porosity of pyroclastic rocks, faults, and fractures. The gangue mineralogy of the stringer veinlets consists of quartz, carbonate, and anhydrite. The distribution of sulfide minerals is zoned vertically and from bottom to top as follows: pyrite - chalcopyrite as disseminations and stringer veinlets; pyrite - sphalerite - chalcopyrite as disseminations, stringer veinlets, and networks; and pyrite - sphalerite - chalcopyrite - tetrahedrite-tennantite - galena as disseminations, stringer veinlets, and massive pods. Hydrothermal alteration assemblages are chloritic alteration, quartz - white mica alteration, propylitic alteration, silicification, argillic alteration, and carbonate alteration. These alteration assemblages display both vertical and lateral zonations. A central zone of chloritic alteration grades laterally into propylitic alteration, and upward into quartz-white mica alteration. The quartz - white mica alteration in turn grades laterally into propylitic alteration. Argillic alteration and carbonate alteration are genetically related but slightly later events that overprint the earlier assemblages.

The mineralization in the Seaman Gulch area is similar to the stockwork zone that underlies Kuroko-type volcanogenic massive sulfide deposits. The sulfides and their associated products of hydrothermal alteration were deposited during submarine geothermal activity that was operative during the latest Permian time.

The economic potential of the Seaman Gulch area is

considered to be low because of the paucity of base metal-bearing sulfides, their occurrence as chiefly disseminations and veinlets, and the restricted distribution of economic assays.

Geology and Mineralization of the Seaman Gulch Area, East Shasta Mining District, Shasta County, California

by

Douglas W. Prihar

A THESIS

submitted to

Oregon State University

in partial fulfillment of
the requirements for the
degree of

Master of Science

Completed February 10, 1987

Commencement June 1988

APPROVED:

Redacted for privacy

Professor of The Department of Geology in charge of major

Redacted for privacy

Chairman of the Department of Geology

Redacted for privacy

Dean of Graduate School

Date thesis is presented February 10, 1987

Typed by Sadie's Word Processing for Douglas W. Prihar

TABLE OF CONTENTS

LIST OF FIGURES

LIST OF TABLES

GEOLOGY AND MINEARLIZATION OF THE SEAMAN GULCH AREA, EAST SHASTA MINING DISTRICT, SHASTA COUNTY, CALIFORNIA

INTRODUCTION

The Seaman Gulch area is located along the southeastern margin of the East Shasta Mining District in the southeastern part of the Klamath Mountains province of northern California. Mining activity in the East Shasta District was sporadic from the turn of the century through 1955. Base and precious metal production have consisted of copper, zinc, lead, silver, and gold from massive sulfide deposits. Exploration activity within the district has been renewed within the past few years. Interest in the geology and economic potential of the Seaman Gulch area was spurred by the discovery of an anomalous base and previous metal-bearing gossan in 1976 by Duval Corporation.

Location and Accessibility

The Seaman Gulch area is located approximately 20 miles (32 km) northeast of Redding, in central Shasta County, California (Fig. 1). The area of study includes approximately two square miles (5.2 km^2), Sec. 8, SW 1/4 Sec. 9, NW 1/4 Sec. 16, and N 1/2 Sec. 17, T. 33 N., R. 2 W., in the Millville, California 15-minute guadrangle.

The study area is accessible from Redding via U.S. Highway 299E. Seaman Gulch Road and Backbone Ridge Road provide access along the western and northern borders of

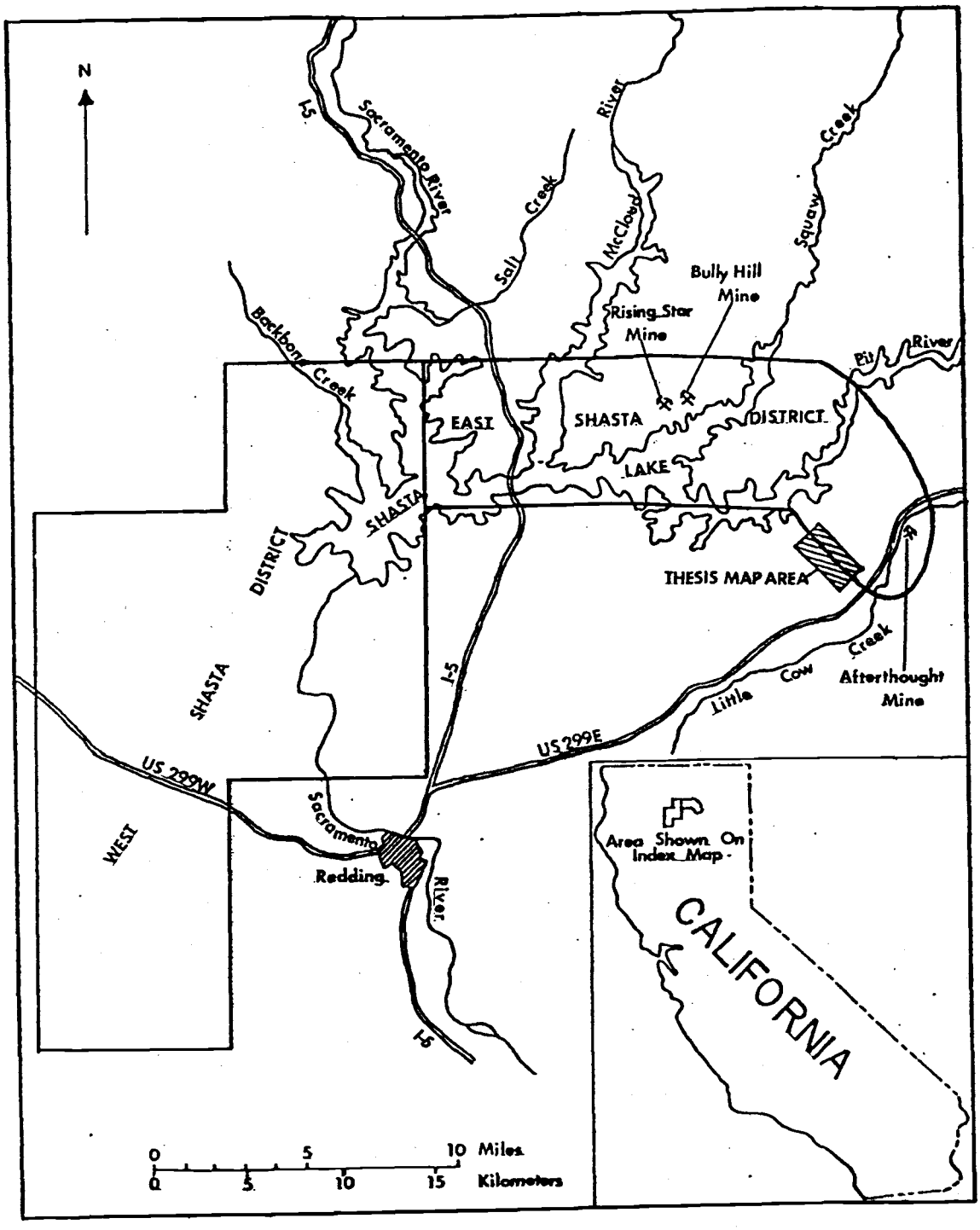

Figure 1. Location map of the East Shasta Mining District and the Seaman Gulch area (modified from Albers and Robertson, 1961).

the area, respectively. Within the Seaman Gulch area, movement is facilitated by private roads and cat-blazes.

Topography, Climate, and Vegetation

The topography of the Seaman Gulch area is that of a partly dissected plain (Albers and Robertson, 1961), with approximately 600 feet (185 m) of relatively gentle relief. Elevations range from slightly more than 1800 feet (554 m) on Backbone Ridge to approximately 1200 feet (369 m) in Seaman Gulch. The relatively flat topography in the vicinity of Seaman Gulch contrasts sharply to that of the maturely dissected, rejuvenated topography generally characteristic of the Klamath Mountains Province.

The climate of the area is characterized by dry, hot summers and cool, wet winters. Temperatures during the summer months range from highs of 80 to 115°F (27 to 43°C) to lows of 50 to 70°F (10 to 21°C). Precipitation averages 62 inches (157 cm) per year (Albers and Robertson, 1961).

A thick vegetative cover is widespread throughout the Seaman Gulch area. Most hill slopes are covered with brush. Manzanita (Arctostaphylos) and western poison oak (*Rhus diversiloba* Torr. & Gray) are the predominant varieties present. Several species of scrub oak and chaparral are other common types of brush present. Small stands of sugar pine (*Pinus lambertiana*), digger pine (*P. sabiniana*) and oak (*Quercus wizlezenii*) are sparsely distributed throughout the area.

Previous Geologic Investigations

Detailed geologic investigations in the Eastern Klamath Subprovince, as defined by Irwin (1966), southeast of the Trinity ophiolite are generally lacking. High relief, thick vegetative cover, limited accessibility, structural complexity, a paucity of distinctive marker units, and overall poor exposure of bedrock have hindered field work in this portion of the Klamath Mountains.

Mining activity near the turn of the century spurred interest in the geology of the East Shasta Mining District and its surrounding area. Initial regional geologic reports and maps (Diller, 1893, 1906; Fairbanks, 1893; Smith, 1894) and subsequent topical studies (Diller, 1903a, 1903b) were published. The most important of these initial works was the Redding Folio (Diller, 1906) which has served as a basis for most of the subsequent work done in the area. The Paleozoic and Mesozoic rocks of the southern Klamath Mountains have been briefly described by Hinds (1932, 1935, 1940), Wheeler (1940), Kinkel and Albers (1956), Coogan (1960), Skinner and Wilde (1965), Murray and Condie (1973), Hilton (1975), Barker and others (1979), Curtis (1983), Fraticelli (1984), Albers and Bain (1985), Lapierre and others (1985), Kistler and others (1985), Bence and Taylor (1985), Miller (1986), Nelson (1986), Miller and Wright (1987), Eastoe and others (1987), and Stevens and others (1987).

Reports on the economic geology of the area were written by Graton (1909) and Boyle (1914), and both described the copper deposits of Shasta County. An extensive examination of the geology and ore deposits of the East Shasta District was published by Albers and Robertson (1961). They concluded that the massive sulfide deposits of the East Shasta District were of an epigenetic-hydrothermal origin. However, Albers (1966) subsequently concluded that these massive sulfide deposits might be of a syngenetic-volcanogenic origin. Moreover, Anderson (1969) mentioned that the alteration mineral assemblages associated with the mines in the East Shasta Mining District are characteristic of those associated with massive sulfide deposits in terrains characterized by greenschist facies regional metamorphism. In addition, Hutchinson (1973) noted that mines of the East Shasta District were of the lead-zinc-copper-silver-type in his classification of massive sulfide deposits of volcanogenic origin; this classification was later modified by Obmoto (1978) to include cauldron subsidence as part of the ore-forming process. Additional detailed studies of the Afterthought Mine, which is located approximately 2 miles (3.2 km) northeast of Seaman Gulch, have been provided by Albers (1953) and Fredericks (1980).

Purpose of the Investigation

The principal purpose of this investigation was to

examine the metavolcanic host rocks, structure, and related sulfide mineralization in detail. Particular attention was directed to the stratigraphic, structural, and alteration environment of the mineralization. A primary or secondary origin for the gossan found in the area was to be determined. The sulfide mineralization was studied in detail to determine whether or not a volcanogenic hypothesis is justifiable, and whether or not the mineralization of this deposit was of an earlier episode than that which characterizes other similar deposits of the East Shasta District. Because the area of concern in this investigation had been previously unmapped, it was hoped that the data gathered might serve as a basis for additional studies of the surrounding area. These objectives were accomplished through detailed field studies of host rock and country rock lithologies, and of their relationships to structure, alteration, and mineralization. Interpretations were supported by appropriate chemical, mineralogic, and petrographic studies of samples collected during the field work.

Methods

Field work was accomplished during a period of five weeks in the spring and two weeks in the fall of 1978, and an additional week in the spring of 1980. The geology of the Seaman Gulch area was mapped at two scales: 1) an enlarged portion (1:12,000) of the Millville, California

15-minute quadrangle as a base map (Plate 1); and 2) a selected area at 1:1200 utilizing plane table methods (Plate 2). Representative samples of the country rocks, wall rock alterations, and mineralization were collected for petrographic, ore microscopic, and whole rock chemical analyses.

Examinations of 66 thin sections and six polished thin sections were made utilizing a Leitz petrographic microscope and ore microscope to identify the major minerals and their textural relationships. The composition of plagioclase feldspars found in the metavolcanic rocks were determined from the low plagioclase feldspar dispersion chart for α' on (001) cleavage flakes found in Ribbe (1975; p. R-55). Refractive indices of individual crystals were determined utilizing standard index oils and a monochromatic sodium light (wavelength = 589 m) source. The Michel-Levy method described by Kerr (1959) was used to determine the composition of plagioclase feldspar in the Tertiary volcanic rocks. Modal analyses were obtained for selected samples using a Leitz mechanical stage and point counter; and 1000 points per thin section were counted.

Major oxide chemical analyses were obtained for ten samples. X-ray fluorescence (SiO_2, TiO_2, Al_2O_3, MgO, Fe_2O_3, and P_2O_5) and atomic absorption spectrometry (Na_2O) analyses were performed at the University of Oregon, Eugene, Oregon.

REGIONAL GEOLOGIC SETTING

The East Shasta Mining District is located in the eastern Klamath lithotectonic belt of Irwin (1966). The eastern Klamath belt is bounded on the east by Cenozoic volcanic rocks of the Cascade province, on the west and north by the central metamorphic belt, and to the south by the Great Valley province (Fig. 2). Rocks of the eastern Klamath belt range from Ordovician through Late Jurassic in age. In general, they form a southwest-trending arch that is complicated by metamorphism, intrusion, and superposed deformation. The core of this arch is defined by the Trinity ophiolite (Fig. 3), a broad mass of ultramafic and gabbroic rocks. The Paleozoic - Mesozoic strata of the eastern Klamath belt are divided into two separate areas by the Trinity ophiolite (Churkin and Eberlien, 1977); these are the Callahan terrane to the northwest and the Redding terrane to the southeast.

Trinity Ophiolite

The Trinity ophiolite is approximately 47 miles (75 km) long and 31 miles (50 km) wide. It consists predominantly of ultramafic and gabbroic rocks, with minor amounts of diabase and volcanic rocks (Linsley-Griffin, 1977). Ordovician U-Pb dates for diorite and layered gabbro range from 455 to 480 m.y.; the U-Pb date for pegmatitic gabbros is 430 m.y. (Mattinson and Hopson, 1972; Hopson and Mattinson, 1973).

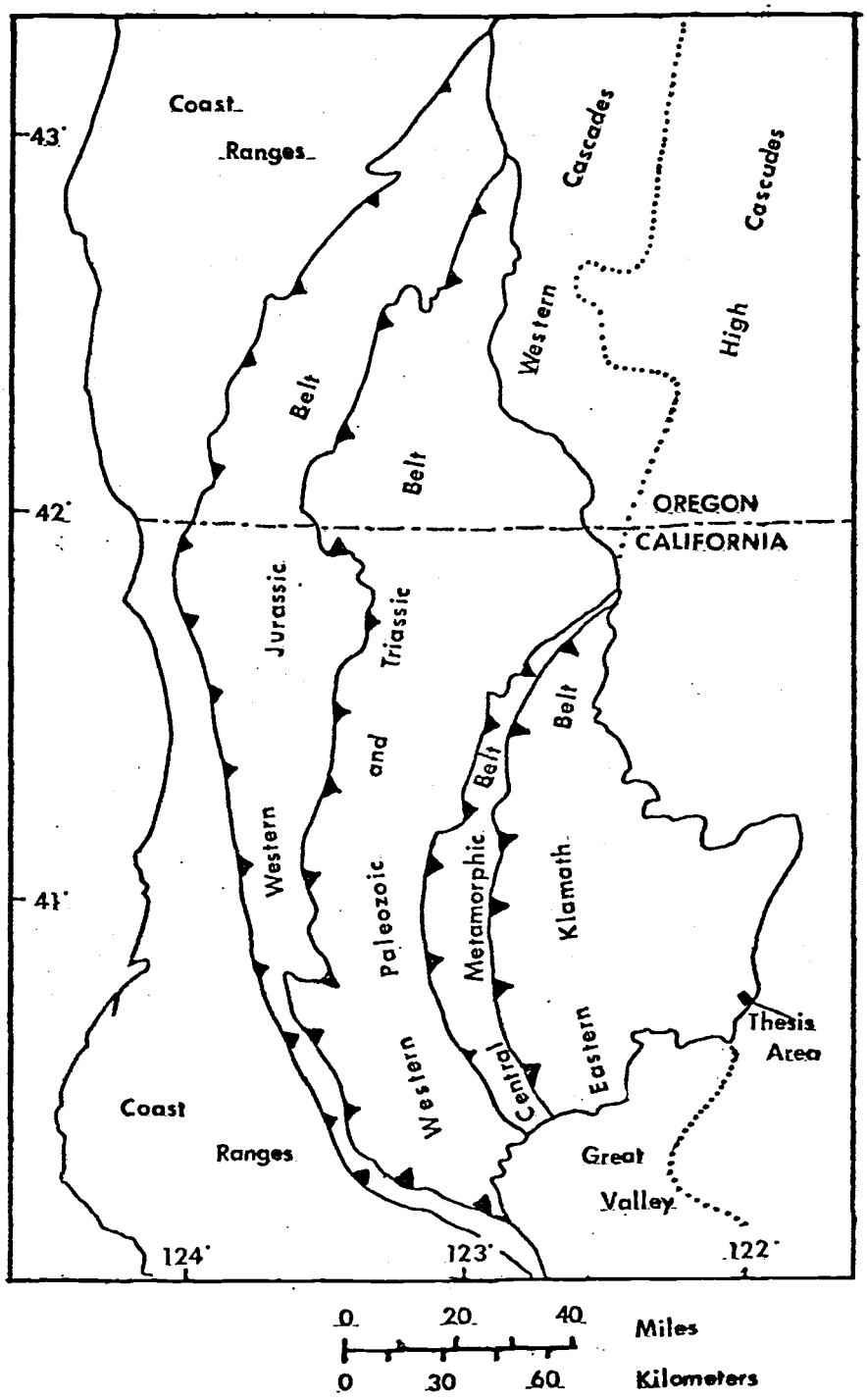

Figure 2. Lithotectonic provinces of the Klamath Mountains.

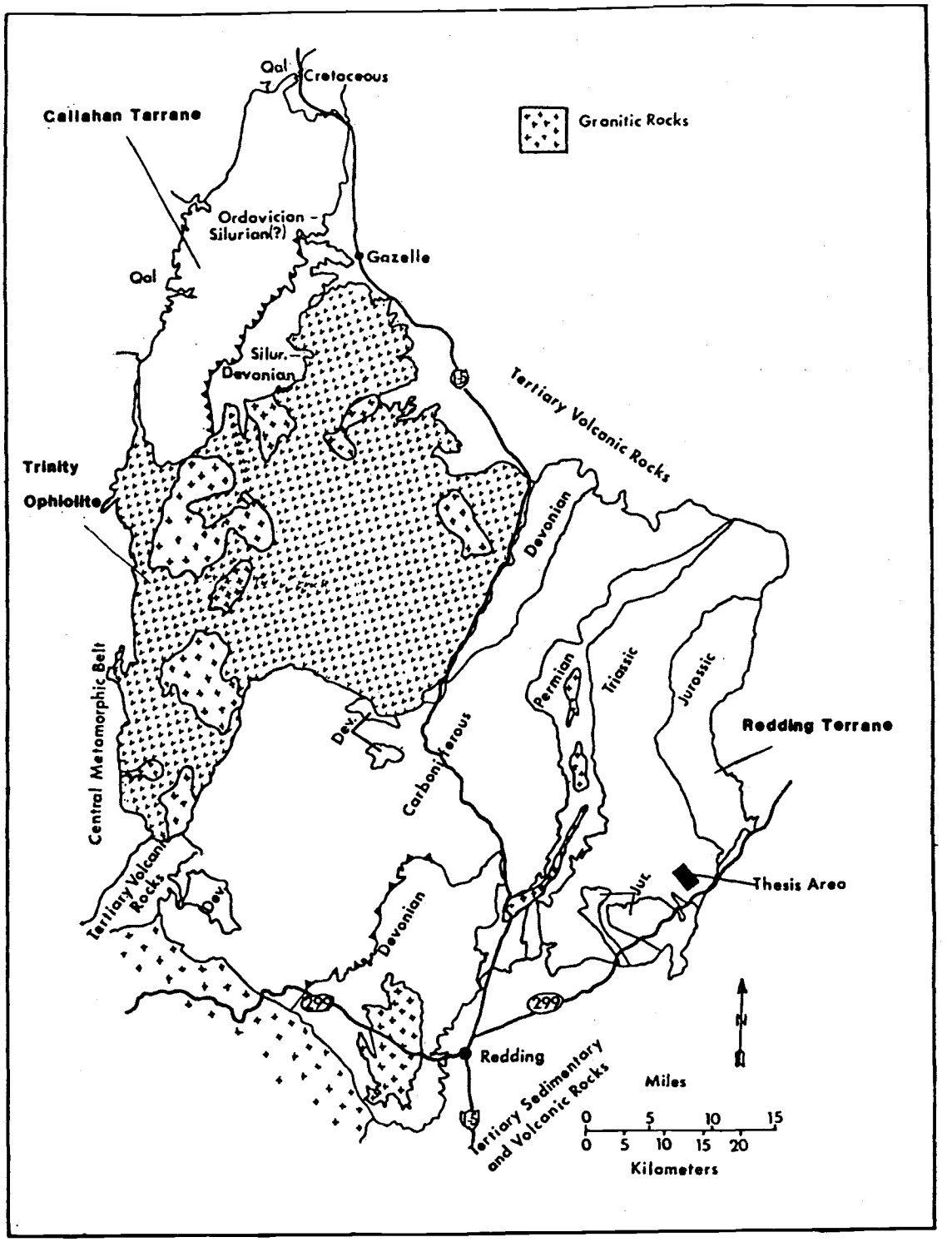

Figure 3. Geologic terranes of the eastern Klamath Subprovince (modified after Lindsley-Griffin, 1977).

On the basis of gravity and magnetic data, the Trinity ultramafic rocks are interpreted to represent a relatively thin, subhorizontal sheetlike mass (Irwin and Bath, 1962; Irwin and Lipman, 1962; LeFehr, 1966), that underlies a large synclinorium of Ordovician to Devonian strata of the Callahan terrane to the northwest (Irwin, 1966; Hotz, 1974). The geophysical data further suggest that the rocks of this sheet may extend some distance to the southeast beneath the younger rocks of the Redding terrane (Griscom, 1977).

Callahan Terrane

The rock units of the Callahan terrane are contained in several thrust sheets and fault slices stacked on top of the Trinity ophiolite. Displacement on some of the faults is thought to be minor, whereas the movement on others was probably large and juxtaposed rock units of similar age but different lithology and depositional history (Potter and others, 1977; Hotz, 1977).

The Gazelle Formation (Wells and others, 1959) has retained its identity in this area although it has been divided into several stratigraphic units. This formation consists of shale, volcanic and arkosic wacke, chert, chert-pebble conglomerate, and some spilite near the base. Rock units of the Gazelle Formation were derived from a calc-alkaline (mainly andesitic) volcanic source (Condie and Snansieng, 1971), range from Early Silurian (?) to

Early Devonian in age, and occupy the southeastern part of the Callahan terrane (Fig. 3).

In contrast, the Duzel Formation of Wells and others (1959) is found to consist of six structural units of uncertain age. The rock units of the Duzel Formation as described by Hotz (1977), Potter and others (1977), and Rohr (1977), are the Sissul Gulch Graywacke, Schulmeyer Gulch sequence, Moffett Creek Formation, Duzel Phyllite, Antelope Mountain Quartzite, and limestone of Duzel Rock. They consist of greywacke, phyllite, quartzite, calcareous and sandy siltstone, shale, quartz arenite, chert, and discontinuous bodies of limestone. According to Condie and Snansieng (1971) the clastic sedimentary rocks of the Duzel Formation are derived from the plutonic-metamorphic terrane. The bulk of the rocks assigned to the Duzel Formation have not been dated paleontologically, and some others are thought to be Silurian in age (Potter and others, 1977). However, other units are known to be Ordovician. Rock units comprising the Duzel Formation occupy the northwestern part of the Callahan terrane (Fig. 3).

Redding Terrane

The Trinity ophiolite (Fig. 3) is overlain to the southwest by east-dipping strata of mafic, intermediate, and silicic volcanic and volcaniclastic rocks of Middle Devonian, Late Mississipian, Pennsylvanian, and possible

Early Permian ages. Overlying these strata are Permian limestone and more arc-type volcanogenic rocks of Late Permian, Triassic, and Jurassic age (Murray and Condie, 1973). Some Devonian to Jurassic basement rocks in the southeastern part of the Redding terrane are overlain unconformably by poorly lithified tuff breccia of Pliocene age (Anderson, 1933; Lydon, 1969) and by basaltic lava flows of Pliocene and(or) Pleistocene age (Albers and Robertson, 1961). The formal rock-stratigraphic units of the Redding terrane, together with their ages, thicknesses, and lithologic descriptions, are listed in Table 1.

Plutonic Rocks

The only known plutons of Paleozoic age in the Klamath Mountains province are the Mule Mountain stock and the Pit River stock. Barker and others (1979), Albers and others (1981), and Kistler and others (1985) have suggested that the Mule Mountain stock is cogenetic with silicic volcanic rocks of the Middle Devonian Balaklala Rhyolite which it intrudes. K-Ar and U-Pb dates of about 400 m.y. from the Mule Mountain stock were obtained by Albers and others (1981). The Pit River stock is exposed along the eastern shores of Lake Shasta and yields K-Ar dates ranging from 251 to 262 m.y. (Hotz, 1971). It is composed of trondhjemite and albite granite. Other plutonic rocks in the eastern Klamath belt include the Shasta Bally batholith, Castle Crags pluton, and several unnamed plutons

which yield K-Ar dates ranging from 127 to 140 m.y. (Davis and others, 1965; Lanphere and others, 1968). These plutons are chiefly diorite to quartz diorite in composition, and exhibit a trondhjemitic differentiation trend (Lanphere and others, 1968).

Table 1. Generalized Stratigraphic Column of the Redding Terrane--Eastern Klamath Belt. (Modified from Irwin, 1966).

Age	Formation	Thickness In Feet	General Features
Quaternary	Unconsolidated Deposits	variable	Includes alluvial material, rock and soil mantle on hill slopes, talus, and landslide deposits.
Pleistocene or Pliocene	Basalt	variable	Small bodies of basalt flows and dikes.
Pliocene	Tuscan Formation	variable	Poorly lithified tuff breccia; interbedded flows, tuff, and basal welded-tuff unit.
Cretaceous	Shasta Bally Batholith and other plutons in the eastern Klamath belt		Tonalite and trondhjemite.
Jurassic	Potem Formation	1000	Argillite and tuffaceous sandstone, with minor beds of pyroclastics, limestone and conglomerate.
	Bagley Andesite	700	Greenstone flow and pryoclastic rocks.
	Arvison Formation	5090	Interbedded volcanic breccia, conglomerate, tuff, and minor greenstone flow rocks.
Triassic	Modin Formation	5500	Volcanic breccias, flows, tuffs, and interbedded sediments; includes Hawkins Creek (breccias, flows, conglomerates), Devils Canyon (limestone, calcareous sediments), and Kosk (breccias, argillites, tuffaceous sandstone) Members.
	Brock Shale	400	Argillite and tuffaceous sandstone
	Hosselkus Limestone	250	Thin-bedded to massive fossiliferous limestone; siliceous in upper part.
	Pit Formation	2000-4400	Predominantly black shale and siltstone, with abundant lenses of metadacite tuff and quartz keratophyre tuff; minor lenses of quartz keratophyre flow rock and fossiliferous limestone.
	Bully Hill Rhyolite	100-2500	Quartz keratophyre flow and pyroclastic rocks, with subordinate hypabyssal intrusive bodies. Includes metadacite, keratophyre and shaly tuff.
	Pit River Stock		Trondhjemite and albite granite.
	Dekkas Andesite	1000-3500	Predominantly greenstone composed of keratophyric and spilitic lava flows and pyroclastic rocks, with some lenses of siliceous mudstone and quartz keratophyre.
Permian	Nosoni Formation	0-2000	Fossiliferous tuffaceous mudstone and tuff with subordinate mafic tuff breccia.
	McCloud Limestone	0-2500	Bedded limestone; locally fossiliferous, siliceous, or dolomitic.
Carboniferous	Baird Formation	3000-5000	Pyroclastic rocks, mudstone, and keratophyric flow rock in the lower part; siliceous mudstone, with minor limestone, chert, and tuff in the middle part; and greenstone, quartz keratophyre, and mafic pyroclastic rocks and flow breccia in the upper part.
	Bragdon Formation	6000	Interbedded shale and mudstone, with grit and chert-pebble conglomerate. Minor pyroclastic rocks and radiolarian chert.
Devonian	Kennett Formation	0-400	Thin-bedded tuff and fossiliferous siliceous mudstone. Small lenses of limestone.
	Mule Mountain Stock		Tonalite and trondhjemite
	Balaklala Rhyolite	0-3500	Quartz keratophyre flows and pyroclastic rocks.
	Copley Greenstone	3700	Keratophyre and spilite flows (including pillow lavas) and pyroclastic rocks; includes minor quartz keratophyre tuff.

STRATIGRAPHIC UNITS

The pre-Tertiary stratigraphic units of the Seaman Gulch area consist of mafic to silicic metavolcanic and sedimentary rocks. Ages of the pre-Tertiary rocks in this area are not well established. The oldest are Upper Permian strata that include the predominantly volcanogenic Dekkas Andesite and Bully Hill Rhyolite. These vocanogenic rocks are overlain by chiefly sedimentary rocks of the Upper Permian to Triassic Pit Formation. The pre-Tertiary units are unconformably overlain by Tertiary volcanic rocks.

Permo-Triassic Basement Rocks

The pre-Tertiary stratigraphic units from oldest to youngest are, in general, the Dekkas Andesite, Bully Hill Rhyolite, and Pit Formation. However, sediments of the Pit Formation locally conformably overlie mafic metavolcanics of the Dekkas Andesite (Silberling and Jones, 1982). Thus, the Bully Hill Rhyolite is not ubiquitous in the pre-Tertiary stratigraphic section throughout the East Shasta District.

Dekkas Andesite

This formation consists of a mixed assemblage of mafic to intermediate volcanics and intercalations of mudstone, tuffaceous sandstone, limestone, and chert. This mixed assemblage was named and described from exposures in Dekkas

Creek by Diller (1906). Additional sections subsequently were measured in Nosoni Creek by Coogan (1960) and along the southern portion of McCloud Lake by Miller (1986). Detailed lithologic, stratigraphic, biostratigraphic, and paleontological descriptions have also been published by Coogan (1960), Albers and Robertson (1961), Miller and Wright (1987), and Stevens and others (1987).

Chlorite schist occurs at the north end of Seaman Gulch and has been interpreted to be correlative with the Dekkas Andesite during this investigation. It is greenish black (5 GY 2/1 to 5 G 2/1) on the fresh surface. Dark greenish gray (5 GY 4/1), dark yellowish brown (10 YR 4/2) and medium gray (N 5) colors dominate the weathered surfaces. This chlorite schist forms shallow, soil covered outcrops on the interstream ridges and upper slopes (Fig. 4), and small cliffs in the stream valleys. Schistosity strikes from N. 60° - 72° W. and dips are steep to the northeast and southwest, or vertical.

The chlorite schist is composed chiefly of fine-grained feathery intergrowths of chlorite, plagioclase feldspar (probably albite), actinolite, and clay minerals with subordinate amounts of calcite, sphene (leucoxene), and epidote. Sparse veinlets of carbonate are contained in the plane of schistosity. In addition, this rock contains abundant subangular to subrounded fragments of amygdaloidal metabasalt in the N½, SE¼, SE¼, Sec. 8. The long axes of these fragments range from 7.5 cm to 20 cm in length and

Figure 4. Shallow outcrop of chlorite schist, N½, SE¼, SE¼, Section 8.

are oriented within the plane of schistosity. These fragments of amygdaloidal metabasalt are almost totally recrystallized, but relict microporphyritic and pilotaxitic textures are preserved. Microphenocrysts of plagioclase feldspar are subhedral to anhedral in crystal form, 0.75 to 2.0 mm in diameter, and have been replaced by psuedomorphic aggregates of albite (An_6 to An_9), chlorite, clay minerals, epidote, carbonate and white mica. The groundmass contains subhedral laths of plagioclase feldspar in subparallel alignment. These laths are less than 0.4 mm in length and are replaced by the same minerals as the microphenocrysts of plagioclase feldspar. The remainder of the groundmass is composed of chlorite, sphene (leucoxene), actinolite, calcite, and Fe-oxides. Amygdules are abundant, prolate to spherical in shape, 0.25 to 33.0 mm in diameter and invariably layered. The major minerals filling these amygdules are chlorite, calcite and clay minerals with subordinate amounts of albite, epidote and quartz. Because the stratigraphic base of this formation is not exposed in the Seaman Gulch area, its thickness could not be determined. However, Albers and Robertson (1961) have estimated the thickness of the Dekkas Andesite to range from 1000 feet to 3500 feet (305 m to 1067 m), Coogan (1960) has measured it to be 3840 feet (1171 m) in Nosoni Creek, and Miller and Wright (1987) and Stevens and others (1987) have reported it to be in excess of 14,760 feet (4500 m) near McCloud Lake.

Age and Origin

Coogan (1960) identified fusulinids and productid brachiopods in this unit as belonging to the Late Permian (early Guadalupian). Albers and Robertson (1961) obtained a late Guadalupian (Capitan) age for the fossils they collected near the base of this formation. In addition, Permian waagenophyllid coral has been described from the top of the Dekkas Andesite by Miller and Wright (1987) and Stevens and others (1987).

The chlorite schist in the Seaman Gulch area is interpreted to represent material that was originally basaltic tuff and basaltic tuff breccia on the basis of relict textures preserved in the coarse fragments. These rocks were subjected to hydrothermal alteration and(or) regional metamorphism. The schistose textures are coincident in space and orientation with fold axes inferred from the geologic map (Plate 1). In addition, undeformed stream cobbles of basaltic tuff breccia were found in Seaman Gulch. Although the source of these cobbles was not discovered, their presence provides additional evidence that the development of schistosity is localized.

Bully Hill Rhyolite

Exposures of silicic lava flows and pyroclastic rocks (quartz keratophyre), and subordinate silicic hypabyssal bodies and intermediate flow rocks (keratophyre) in the

vicinity of Bully Hill were given the name Bully Hill Rhyolite by Diller (1906). This formation is economically important, as it hosts the volcanogenic massive sulfide deposits in the East Shasta Mining District.

Previous workers in the district (Diller, 1906; Albers, 1953, 1959; Albers and Robertson, 1961; and Fredericks, 1980) have used rhyolite and andesite interchangeably with quartz keratophyre and keratophyre, respectively. They have documented that albite has psuedomorphically replaced plagioclase feldspar; and, thus, these metavolcanics are quartz keratophyre and keratophyre. However, Albers and Robertson (1961) have identified some silicic metavolcanics in which primary plagioclase feldspar shows only partial replacement by albite. They refer to these rocks as metadacite. This latter example is typical of the silicic metavolcanics from the Seaman Gulch area, where the anorthite content of plagioclase feldspar ranges from An_3 to An_{25}. Hence, metadacite is used during this investigation because it better describes silicic metavolcanic rocks in the Seaman Gulch area. Thus, the most common lithologies of this unit are metadacitic pyroclastics, flows or domes, and hypabyssal rocks. Subordinate amounts of metabasaltic andesite and an altered mafic intrusion are also present.

The thickness of the Bully Hill Rhyolite varies from 100 to 2500 feet (300 to 760 m) according to Albers and Robertson (1961). The thickness in the Seaman Gulch area

is approximately 225 feet (73 m). This estimate of thickness was determined from the north end of Seaman Gulch.

Metadacitic Pyroclastic Rocks

Metadacitic pyroclastic rocks comprise the bulk of the Bully Hill Rhyolite. These rocks are grayish green (10 G 4/2), grayish olive green (5 GY 3/2), dark greenish gray (5 G 4/1), light bluish gray (5 B 5/1), and bluish white (5 B 9/1) on their fresh surfaces and vari-colored on the weathered surfaces. They crop out as shallow, subdued exposures (Fig. 5) or rubbly mounds. The metadacitic pyroclastics have been classified according to the terminology of Fisher (1961, 1966) and consist chiefly of lithic lapilli tuff and pumiceous crystal tuff with subordinate amounts of vitric (?) tuff, lithic lapillistone, and lithic tuff breccia. The clasts are chiefly angular to subrounded and poorly to moderately sorted lithic fragments of porphyritic metadacite (50.5 to 81.3 percent), leucocratic plutonic rock, possibly trondhjemite (4.4 to 9.0 percent), pumice (trace amounts to 0.7 percent) and fossil fragments (trace amounts) that have been replaced by pyrite. These clasts range from 2 to 220 mm in diameter and are set in a matrix of altered vitric (?) material (12.6 to 31.1 percent) and crystal fragments that are chiefly quartz (1.1 to 11.2 percent), plagioclase feldspar (1.5 to 9.6 percent), pyrite (0.3 to 1.8 percent) and trace amounts of apatite, zircon, leucoxene, hematite and goethite.

Secondary minerals formed by alteration and(or) metamorphism of these pyroclastics include feldspar (probably albite), quartz, white mica, calcite, chlorite and smectite.

Foliation, poorly to well developed, is invariably present and strikes from N. 38° W. to N. 82° E. and dips steeply to the northeast or southwest. The metadacitic pyroclastics with well-developed foliation (Fig. 6) are only found adjacent to faults and within a few feet of the fault grade into pyroclastics that have poorly developed foliation. In addition, the strongly foliate pyroclastics are invariably altered to an assemblage of smectite with subordinate amounts of quartz and white mica. The spatial coincidence of intense alteration and well-developed foliation in the pyroclastics with faults suggests that hydrothermal activity and structural activity were largely contemporaneous.

Sparse stratification is manifest as alternating light and dark laminae (1 to 8 mm thick) in vitric (?) tuff (Fig. 7) and crude normal graded beds from 3 to 70 feet (0.9 to 21.3 m) thick. However, the bulk of the metadacitic pyroclastics are massive.

Porphyritic Metadacite

Porphyritic metadacite is interbedded with or intrudes the metadacitic pyroclastics. It crops out as blocky masses and is medium light gray (N 6), dark greenish gray

Figure 6. Schistose metadacitic lithic lapilli tuff.

Figure 7. Laminated vitric (?) tuff from diamond drill hole 1 - 144 feet. Note the slightly discordant vein of sulfide at the bottom of the photo.

(5 G 4/1), or greenish gray (5 GY 7/4) in color. Columnar joints are erratically distributed and consist of 4-, 5-, and 6-sided prisms with cross-sectional diameters averaging 5 inches (12 cm), (Fig. 8). In addition, the columnar joints occur in linear to sinous clusters whose margins are commonly fragmental.

Porphyritic metadacite contains glomerocrysts and phenocrysts of plagioclase feldspar (10.1 to 12 percent) with quartz (0 to 4 percent). These glomerocrysts and phenocrysts are set in a dense, siliceous groundmass. Modal analyses of porphyritic metadacite are listed in Table 2.

Petrographically, the glomerocrysts and phenocrysts of plagioclase feldspar are subhedral, from 2 to 10 mm in length, and are albite to oligoclase (An_3 to $_{25}$) in composition. Alteration products of plagioclase feldspar are chiefly clay minerals, epidote, carbonate, and subordinate amounts of white meca, and quartz. The phenocrysts of quartz are euhedral to subhedral in crystal form, 1 to 4 mm in diameter, and embayed. The groundmass consists of a microcrystalline mosaic of quartz-feldspar (possibly albite) - clay minerals (68.2 to 77.6 percent) and varying amounts of calcite, Fe-Ti oxide, sphene (leucoxene), and pyrite. In addition, microspherulites are found in the groundmass. Moreover, sparse amygdules are present and have been filled by granoblastic quartz with inclusions of green acicular crystals that are possibly actinolite.

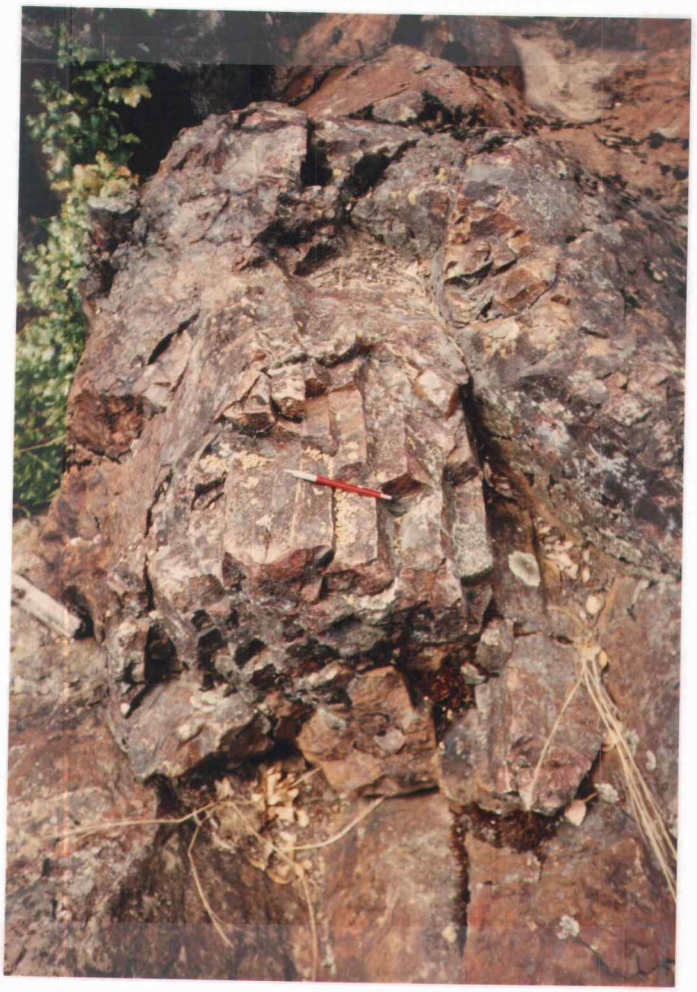

Figure 8. Prismatic columnar joints in porphyritic metadacite in Seaman Gulch.

Table 2. Modal Analyses of Porphyritic Metadacite and Metabasaltic Andesite

	(percent) DP-80-78[1]	DP-20-78[2]	DP-73-78[2]	DP-45-78[3]
Phenocrysts:				
Plagioclase Feldspar	12	10.1	11.4	TR
Quartz	4	-	-	-
Groundmass:				
Microcrystalline quartz-feldspar-clay	77.6	74.1	68.2	76.3
Chlorite	3.2	11.3	10.2	5.6
Epidote	0.4	2.3	4.1	0.7
Carbonate	1.7	1.4	4.6	15.5
Sphene(leucoxene)	0.7	0.3	0.9	-
Fe-Ti oxide	-	0.1	0.3	-
White mica	TR	-	-	0.2
Granoblastic quartz	-	0.4	0.2	0.8
Pyrite	0.3	-	-	0.9
Total:	99.9	99.5	100	100

TR - Indicates trace amounts.

1 - Porphyritic metadacite with glomerocrysts and phenocrysts of plagioclase feldspar and quartz.

2 - Porphyritic metadacite with glomerocrysts and phenocrysts of plagioclase feldspar

3 - Metabasaltic andesite

Metabasaltic Andesite

Metabasaltic andesite is volumetrically minor. It is similar to porphyritic metadacite in color and outcrop expression. The textures in hand specimen are nonporphyritic and amygdaloidal. Metabasaltic andesite occurs as elliptical lobes that are 20 to 80 feet (6.5 to 24.4 m) thick. Petrographically, this rock contains trace amounts of microphenocrysts of plagioclase feldspar that are set in an altered groundmass that consists chiefly of an anhedral microcrystalline mosaic of quartz-feldspar (possibly albite) - clay minerals that have been partially replaced by carbonate (15.5 percent), chlorite (5.6 percent), epidote (0.7 percent), pyrite (0.9 percent), and white mica (0.2 percent). Amygdules are filled by granoblastic quartz and calcite. Modal mineral percentages of metabasaltic andesite are listed in Table 2.

Altered Intrusive Basalt

An altered basalt intrudes metadacitic pyroclastics in the SW¼, NW¼, NW¼, Sec. 16 and SE¼, NE¼, NE¼, Sec. 17. It is greenish black (5 GY 2/1) to dark greenish gray (5 GY 4/1) in color and crops out as shallow, blocky masses. Columnar joints are common and manifest as 5- and 6-sided prismatic columns that are 8 to 12 inches in diameter (Fig. 9). This altered intrusive basalt is nonporphyritic and amygdaloidal. Contact relationships with the

metadacitic pyroclastics are sharp where observed. The western contact of this intrusion was intersected by a diamond drill hole and it is brecciated. The breccia contains fragments of altered basalt and rarely metadacite that are angular, up to 18 cm in diameter, and cemented by calcite (Fig. 10). Similar altered mafic dikes intrude analogous rocks at the Bully Hill Mine, according to Albers and Robertson (1961). Petrographically, the altered intrusive basalt contains microphenocrysts of plagioclase feldspar and clinopyroxene that are 0.75 to 1.5 mm in diameter. Alteration of these microphenocrystic phases is ubiquitous. Plagioclase feldspar has been partially to completely replaced by chlorite near the center of the intrusion and to calcite-chlorite along the margins. Clinopyroxene similarly displays partial to complete replacement by chiefly chlorite and subordinate amounts of sphene (leucoxene) and clay minerals in the center of the intrusion with calcite and chlorite being the chief products of alteration along the margins. The groundmass of this altered intrusive basalt consists of relict subhedral laths of plagioclase feldspar that are partially to completely replaced by smectite, carbonate, chlorite, and epidote. The minerals interstitial to the altered laths of plagioclase feldspar are chiefly Fe-Ti oxide, sphene (leucoxene), chlorite, calcite, and subordinate amounts of epidote, smectite and white mica. In addition, remnant anhedra of clinopyroxene, 0.4 mm in diameter, are found in

Figure 9. Cross-sectional view of columnar joints in altered intrusive basalt.

Figure 10. Breccia from the western margin of the intrusion of altered basalt. Calcite cements the breccia and fills amygdules in the angular fragments of altered basalt. Diamond drill hole 3 - 158 feet.

the groundmass. The texture of the groundmass is intersertal near the center of the intrusion and pilotaxitic along the margins. Amygdules are filled by chlorite and calcite.

Banded Metadacite Breccia

Banded metadacite breccia crops out in the SW¼, NE¼, NE¼, Sec. 17 and was mapped separately from the other metadacitic pyroclastics because of its unique assemblage of clasts and apparent contact relationships with the adjacent rocks. This breccia is commonly greenish gray (5 GY 7/4) and is composed chiefly of angular fragments of banded metadacite and subordinate amounts of porphyritic metadacite (Fig. 11). The contacts are obscured, but they appear to cut across the general structural grain interpreted to be present in the adjacent metadacitic pyroclastics. Thus, this breccia is hypothesized to be possible vent fill material.

Petrographically, the banded metadacite fragments are nonporphyritic and pervasively altered, chiefly to quartz, clay minerals, plagioclase feldspar (possibly albite), and subordinate amounts of chlorite and Fe-Ti oxide. The fragments of porphyritic metadacite and the material comprising the matrix are similar to those described previously for the metadacitic pyroclastics.

Figure 11. Banded metadacite breccia from the SW¼, NE¼, NE¼, Sec. 17.

Gossan

Gossan crops out along the margin of the altered intrusive basalt and it was mapped as a separate unit on Plate 2. It represents the oxidized equivalent of mineralized metadacitic pyroclastic rocks that were intersected at depth by diamond drill holes. The occurrence and formation of this gossan is discussed in the chapter on Economic Geology.

Chemical Composition

Two samples of porphyritic metadacite, one sample of metabasaltic andesite, and two samples of altered intrusive basalt were analyzed for their major and minor element abundances in an attempt to establish their representative compositions. The chemical compositions and the CIPW normative mineralogy are presented in Tables 3 and 4, respectively. The petrography of metadacite and metabasaltic andesite were given previously in Table 2. For comparison, chemical analyses of spilite, keratophyre, and quartz keratophyre from the Dekkas Andesite and Bully Hill Rhyolite (Albers and Robertson, 1961; Fredericks, 1980), the average spilite (Vallance, 1969), the average island arc tholeiite series basalt (Jakes and White, 1972), basaltic andesite from Tonga (Ewart and others, 1973), average dacite (LeMaitre, 1976), and dacite from Tonga (Ewart and others, 1973) are listed in Table 3.

Table 3. Major Oxide (percent) and Trace Element (ppm) Analyses

Table 3. Major oxide(percent) and trace element (ppm) analyses

	1	2	3	4	5	6	7	8	9	10	11	12	13	14	15
SiO_2	48.83	49.55	56.83	68.31	72.06	52.30	65.52	71.92	70.45	72.83	49.00	51.57	54.51	65.01	66.26
TiO_2	0.86	0.84	1.19	0.52	0.23	0.64	0.47	0.11	0.36	0.35	1.50	0.80	0.60	0.58	0.59
Al_2O_3	16.68	16.64	16.62	13.74	13.88	17.60	14.90	13.24	14.47	12.77	15.40	15.91	15.84	15.91	14.18
FeO*	14.02	13.37	9.65	7.64	4.02	8.90	7.80	4.76	3.32	3.70	7.95	9.78	10.85	4.73	8.06
MnO	0.19	0.17	0.22	0.20	0.07	0.16	0.05	0.07	0.05	0.04	0.18	0.17	0.20	0.09	0.19
MgO	5.28	5.32	2.91	1.42	0.79	6.40	1.10	0.91	1.38	1.45	5.30	6.73	4.93	1.78	1.64
CaO	8.96	9.29	2.44	1.36	0.83	2.80	0.64	0.26	0.85	2.07	7.60	11.74	10.25	4.32	5.73
Na_2O	2.28	2.47	5.32	5.94	5.97	6.20	4.85	6.45	5.99	4.38	4.10	2.41	1.69	3.79	2.79
K_2O	0.48	0.34	0.10	0.03	1.19	0.15	1.97	0.04	1.70	0.80	1.10	0.44	0.56	2.17	1.03
P_2O_5	0.04	0.03	0.24	0.13	0.04	0.16	0.16	0.14	0.10	0.10	0.30	0.11	0.09	0.15	0.21
TOTAL	97.62	98.01	95.53	99.28	99.08	95.36	97.46	99.67	98.89	98.67	95.33	99.66	99.65	98.53	100.68
							TRACE ELEMENTS (ppm)								
As	0.7	0.4	0.7	0.4	0.3										
Cu	110	70	30	18	15										
Mo	1	-1	3	2	3										
Pb	16	14	25	9	7										
Zn	55	55	100	75	35										
Sp. Grav.	2.71	2.71	2.67	2.65	2.66	2.68	2.65		2.66	2.66					

Sample explanation: 1 and 2 - altered intrusive basalt (DP-9 and 36-78, respectively); 3 - metabasaltic andesite (DP-45-78); 4 - porphyritic metadacite with phenocrysts of plagioclase feldspar (DP-20-78); 5 - porphyritic metadacite with phenocrysts of quartz and plagioclase feldspar (DP-80-78); 6 - spilite(Albers and Robertson, 1961); 7 - kerate phyre (Albers and Robertson, 1961); 8 - keratophyre (Fredericks, 1980); 9 and 10 - quartz keratophyre (Albers and Robertson, 1961); 11 - average spilite (Vallance, 1969); 12 - average island arc tholeiite series basalt (Jakes and White, 1972); 13 - basaltic andesite from Tonga (Ewart and others, 1973); 14 - average dacite (LeMaitre, 1976); and 15 - dacite from Tonga (Ewart and others, 1973).

* - Total iron

The classification of metavolcanic rocks is based on complementary mineralogic and compositional criteria. However, these criteria may not be strictly applicable when rocks have been modified by a variety of alteration, metamorphic, and tectonic processes which change the primary mineralogy and mobilize the major element components. The mineralogical and compositional data in Tables 2, 3, and 4 clearly indicate that the metavolcanic rocks from Seaman Gulch have been modified in their mineralogy and composition, but these analyses represent the least altered rocks available.

Porphyritic metadacite from the Seaman Gulch area is chemically similar to analyses of keratophyre and quartz keratophyre reported by Albers and Robertson (1961) and Fredericks (1980) from the East Shasta District. Specifically, porphyritic metadacite with phenocrysts of quarts and plagioclase feldspar is similar in major element composition to quartz keratophyre (type-1 quartz keratophyre of Schermerhorn, 1973), and porphyritic metadacite with phenocrysts of plagioclase feldspar shows a close correspondence in bulk composition with those rocks described as keratophere (type-2 quartz keratophyre of Schermerhorn, 1973). Thus, dacite is the likely protolith of keratophyre and quartz keratophyre in the East Shasta District. Chemical analysis of porphyritic metadacite with phenocrysts of plagioclase feldspar shows enrichments of SiO_2 and Na_2O and depletions of CaO and K_2O relative to

Table 4. CIPW Normative Analyses (weight percent)

	1	2	3	4	5
Cor	0	0	4.1	1.8	1.4
Qz	4.6	4.7	14.6	26.8	28.9
Or	2.9	2.1	0.6	0.2	7.1
Ab	19.9	21.5	47.4	50.9	51.1
An	35.0	34.3	11.1	5.9	3.9
Hy	19.5	18.1	14.0	9.1	4.9
Di	8.7	10.6	0	0	0
Ap	0.1	0.1	0.6	0.3	0.1
Il	1.7	1.6	2.4	1.0	0.4
Mt	7.4	7.0	5.2	3.9	2.1

Numbers 1 through 5 correspond to those similarly numbered in Table 3.

dacite from Tonga (Ewart and others, 1973) and average dacite of LeMaitre (1976).

Chemical analysis of metabasaltic andesite shows enrichments of SiO_2 TiO_2, Al_2O_3, and Na_2O and depletions of FeO (total), MgO, CaO, and K_2O as compared to basaltic andesite from Tonga. Altered intrusive basalt is texturally similar in hand specimen to spilite from the Dekkas Andesite; however, there are substantial differences in the concentrations of their major oxide components. The altered intrusive basalt shows enrichments of TiO_2, FeO (total), CaO, and K_2O and depletions of SiO_2, Al_2O_3, MgO, Na_2O, and P_2O_5 as compared to the spilite. These contrasts in composition are interpreted to reflect the different conditions that prevailed during alteration of these rocks. The intrusion of basalt was intensely altered by hydrothermal fluids to chlorite- and carbonate-rich assemblages, whereas, the spilite contains products of alteration such as chlorite-calcite-epidote-clay minerals-plagioclase feldspar (probably albite) $\pm$ actinolite $\pm$ pumpellyite (Albers and Robertson, 1961) that are more typical of ocean floor and (or) low grade regional metamorphism. In contrast, the altered intrusive basalt is more closely similar in composition to the average island arc tholeiite series basalt of Jakes and White (1972). Both contain similar concentrations of TiO_2, MnO, Na_2O, and K_2O; although the altered intrusive basalt shows enrichments of Al_2O_3 and FeO (total) and depletions of SiO_2, MgO, CaO, and

P_2O_5 relative to the average island arc tholeiite. In general, chemical compositions indicate Na_2O addition and K_2O and CaO loss due to hydrothermal alteration and (or) ocean floor metamorphism.

It is impossible to determine the magmatic affinity of the metavolcanic rocks comprising the Bully Hill Rhyolite on the basis of major element composition. The significant major oxides such as the alkalis and lime cannot be considered because of the extent to which they have been enriched or depleted due to their likely mobility during alteration and (or) metamorphism. Thus, the metavolcanic rocks comprising the Seaman Gulch area are compositionally typical of island arc volcanism, but probably subsequently modified by ocean floor and (or) geothermal (hydrothermal) metamorphism.

Age and Origin

Faunal and radiometric ages of the metavolcanic rocks comprising the Bully Hill Rhyolite are lacking. Thus, an estimate of the age of this formation is made on the basis of its concordant stratigraphic position between the underlying Dekkas Andesite (Late Permian) and the overlying Pit Formation (Late Permian to Triassic). Because the top of the Dekkas Andesite is Late Permain (Coogan, 1960; Miller and Wright, 1987) and the base of the Pit Formation locally has been assigned a Late Permian age by Silberling and Jones (1982), the Bully Hill Rhyolite is probably also late

Permian in age. The Bully Hill Rhyolite was assigned a Permo-Triassic age by Watkins and Stensrud (1983) on the basis of comparatively similar strategraphic relationships.

The metavolcanic rocks comprising the Bully Hill Rhyolite are the products of submarine volcanism. A submarine environment of deposition has been established for the underlying Dekkas Andesite (Coogan, 1960; Albers and Robertson, 1961) and the overlying Pit Formation (Albers and Robertson, 1961). In addition, the volcanogenic massive sulfide deposits in the East Shasta District were precipitated at the Bully Hill - Pit contact and confirm a submarine environment of deposition for the stratigraphic top of the Bully Hill Rhyolite.

Metadacitic pyroclastics are composed chiefly of poorly sorted, angular to subrounded fragments of lithic, pumice and crystals that occur in thick, discontinuous massive to slightly graded beds. These textures are similar to rocks deposited by subaqueous debris flows or the subaqueous pyroclastic flow deposits of Fiske (1963) and Fiske and Matsuda (1964). Debris flows such as these are the products of phreatic and phreatomagmatic eruptions beneath a column of water. Seawater, in such cases, continuously entered the volcanic vents, explosively flashed to steam upon contact with hot rock or magma, and consistently communited rock in the throat of the vent. In addition, any domes or spines would be explosively disintegrated as they were extruded into sea water. Thus,

large volumes of comminuted rock and (or) subordinate amounts of juvenile material accumulated near the vents, where they became saturated and intermittently collapsed, and were subsequently transported down the flanks of the submerged volcanoes as debris flows, or possibly subaqueous pyroclastic flow deposits similar to those described by Fiske and Matsuda (1964) and Bond (1973).

The porphyritic metadacites and metabasaltic andesites occur as lobate bodies that commonly contain columnar joints. The margins of clusters of columnar joints in these rocks are brecciated and grade into lithic lapilli tuff that contain heterolithic fragments of metadacite. The origin of the lobes of porphyritic metadacite is possibly analogous to that proposed for subaqueous (subglacial) rhyolite flows or intrusions into water-saturated pyroclastics by Furnes and others (1980). However, the lobes of porphyritic metadacite and metabasaltic andesite lack obvious chilled margins as might be expected if molten rock were injected into water-saturated pyroclastics. If the lobes are rootless, then alternatively, they may be large blocks carried by debris flows and (or) blown from vent areas during phreatic eruptions as described in the preceding paragraph. Megabreccias with blocks as large as 1000 to 2000 m in size are found near the base of the Pit Formation according to Eastoe and others (1987). They interpreted the megabreccias to be olistostromes that were deposited by one or more large debris flows.

Pit Formation

The Pit Formation consists chiefly of shale, mudstone, and pyroclastic rocks, and subordinate amounts of siltstone, limestone, and metadacite, according to detailed lithologic descriptions by Albers and Robertson (1961) and Fredericks (1980). This formation was named by Fairbanks (1894) for exposures along the Pit River, although no type-locality was indicated. Diller (1906) restricted the Pit Formation to sedimentary and pyroclastic rocks lying above the Dekkas Andesite and (or) the Bully Hill Rhyolite and beneath the Hosselkus Limestone. The contact between the Pit Formation and Bully Hill Rhyolite is placed at the lowermost bed of shale.

Carbonaceous tuffaceous shale and interbeds of metadacitic lithic lapilli tuff overlie the Bully Hill Rhyolite in the SE¼ NW¼; SW¼ NE¼; and NW¼ SW¼; Sec. 8 and form shallow exposures in stream valleys. Shale is grayish black (N 4) and is thinly bedded or contains chaotic structure indicative of soft-sediment slumping (Figs. 12 and 13), whereas the interbeds of metadacitic lithic lapilli tuff are grayish green (10 GY 4/2) and consist chiefly of poorly sorted, subangular to subrounded fragments of metadacite and minor amounts of elongate, angular fragments of shale. These interbeds of lithic lapilli tuff are 2 to 8 feet (0.61 to 2.44 m) thick, although, they individually lack internal stratification. The fragments

Figure 12. Thinly bedded carbonaceous tuffaceous shale from the north end of Seaman Gulch.

Figure 13. Shale of the Pit Formation showing a disrupted texture.

of porphyritic metadacite range from 2 to 33 mm in diameter and those of shale are 2 to 6 mm in length. The matrix is siliceous, dense and contains crystal fragments of quartz and plagioclase feldspar (possibly albite).

Petrographically, the shale is composed of anhedral microcrystalline quartz (possibly volcanic glass or pumice in part), dark brown carbonaceous material, white mica and subordinate amounts of chlorite, leucoxene, and angular to subangular grains of quartz that are less than 0.25 mm in diameter (fine to very fine sand). Metadacitic lithic lapilli tuff contains fragments of porphyritic metadacite, some with trachytic texture, and shale in a matrix of microcrystalline anhedra of quartz-feldspar (possibly albite)-chlorite and minor amounts of white mica, calcite and leucoxene.

The thickness of the Pit Formation is difficult to determine because the shales in the Seaman Gulch area are closely folded. However, Diller (1906) has estimated the thickness of this formation to be in excess of 2,000 feet (610 m) and Albers and Robertson (1961) suggest a thickness of about 5,000 feet (1,524 m).

Age and Origin

Albers and Robertson (1961) have defined the age of the Pit Formation as Middle to Late Triassic on the basis of faunal evidence. Subsequently, Silberling and Jones (1982) dated the basal portion of this formation as Late

Permian in age from radiolarians in beds of chert along Nosoni Creek. Thus, they inferred the presence of a depositional hiatus covering the duration of Early Triassic time within the Pit Formation. Eastoe and others (1987) have recently documented the presence of a large olistostrome in the lower part of the Pit Formation near Shasta Lake that appears to be of Middle Triassic age. Thus, the formation of this Middle Triassic olistostrome may account for the apparent Early Triassic stratigraphic gap that was noted by Silberling and Jones (1982).

Deposition of thinly bedded shales that characterizes the Pit Formation marks the onset of clastic sedimentation that began during the waning stages of silicic volcanism. Some of the shales near the base of this formation exposed at the north end of Seaman Gulch exhibit chaotic textures. They occupy the same stratigraphic position as the olistostrome described by Eastoe and others (1987) near Shasta Lake, and thus may indicate the presence of an olistostrome in the Seaman Gulch area. Possible mechanisms for the formation of the chaotic textures and (or) olistostrome may include: deposition on initially steep slopes with resulting gravity-induced slumping; deposition near an active fault scarp with seismic-induced slumping; or deposition on the flank of a volcano with subsequent disruption occurring in response to powerful phreatic eruptions. Eastoe and others (1987) favor the formation of the olistostrome and debris flow deposits throughout the Triassic and

Upper Permian to be the product of seismically triggered slumping along a fault scarp that was formed and was rendered unstable by rifting.

The interbeds of metadacitic lithic lapilli tuff are interpreted to have been deposited by debris flows on the basis of their similarities to analogous rocks in the underlying Bully Hill Rhyolite. The presence of clasts of shale in these pyroclastics is evidence that these debris flows were erosional. Moreover, according to Fisher and Schmincke (1984) shale fragments are frequently found in subaqueous pyroclastic flow deposits. Eastoe and others (1987) have provided evidence to support a debris flow origin for interbeds of metadacitic lithic lapilli tuff near Shasta Lake.

Tertiary Stratigraphic Units

Tuscan Formation

The oldest Tertiary unit in the Seaman Gulch area is the Tuscan Formation. The Tuscan Formation consists chiefly of tuff breccia, lapilli tuff and volcanic conglomerate, sandstone, and siltstone. Subordinate rock types include rhyodacitic ashflow tuff, flow breccia, flows of andesite or basalt, and claystone. Tuff breccias comprise 75 percent of the formation (Lydon, 1969). The type section for the Tuscan Formation was designated by Diller (1906) to be located at Tuscan Springs, approximately 12 miles (9 km) northeast of Red Bluff (Fig. 14).

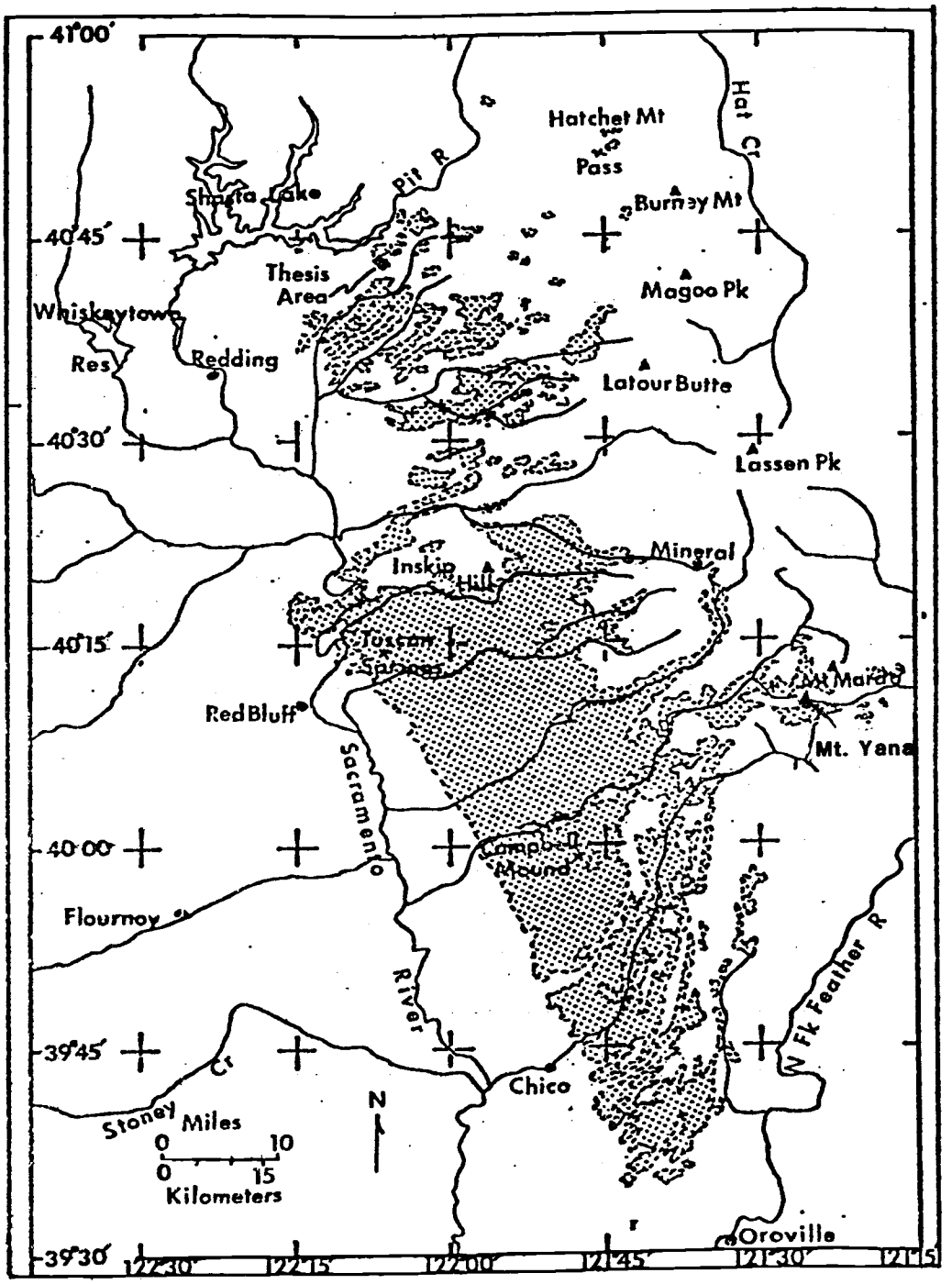

Figure 14. Areal distribution of the Tuscan Formation near Redding, California (modified from Lydon, 1969)

Field Description

The Tuscan Formation was found to consist entirely of poorly consolidated tuff breccia in the Seaman Gulch area. The tuff breccia contains angular to subrounded lithic blocks and lapilli that are erratically distributed in a very pale orange (10 YR 8/2), poorly sorted, friable, tuffaceous matrix (Fig. 15). The lithic fragments are chiefly andesite, with subordinate amounts of dacite porphyry, basalt, and metavolcanics. Discernible bedding features in the Tuscan Formation are absent.

Erosion of the Tuscan Formation produces rounded ridge tops whose surfaces are covered by a residual rubble of block-size clasts. The rubble is the result of the removal of the finer matrix material during erosion and the concentration of the larger blocks on the surface.

The thickness of the Tuscan Formation in the Seaman Gulch area ranges from 20 to 80 feet (6 to 24 m). The formation overlies the pre-Tertiary basement rocks with marked unconformity.

Age and Origin

The age of the Tuscan Formation is generally taken to be Late Pliocene. Direct evidence supporting a Late Pliocene age comes from the Nomlaki Tuff Member (a rhyodacitic welded tuff) of Russell and VanderHoff (1931). A K-Ar date of 3.3 m.y. was obtained by Everndon and others

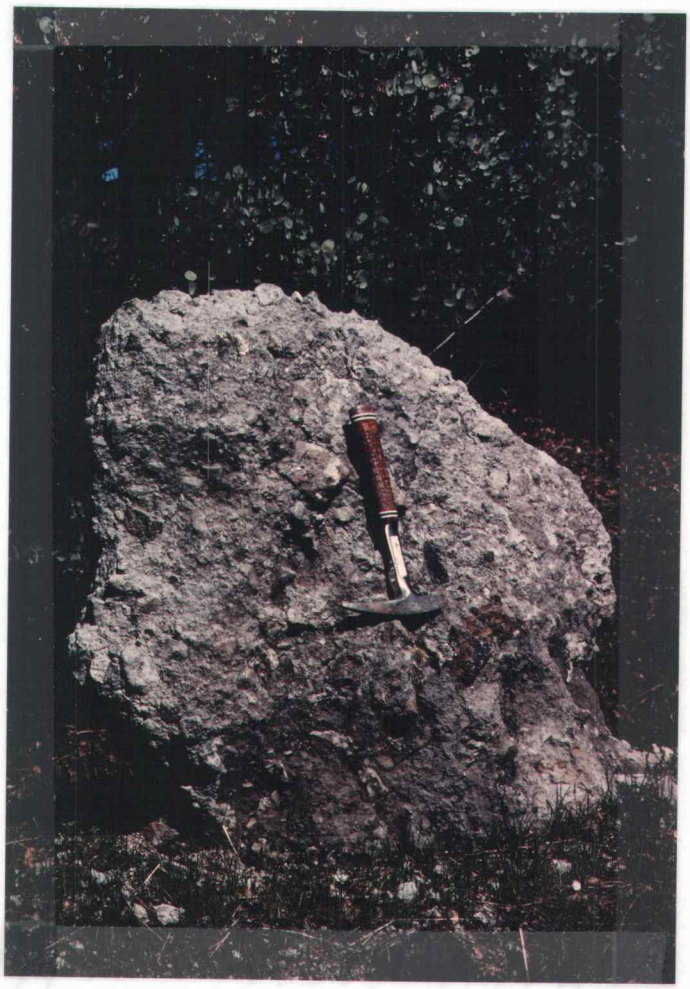

Figure 15. Erosional remnant of a lahar from the Tuscan Formation.

(1964) for the Nomlaki Tuff. Indirect evidence supporting the Late Pliocene age comes from the Tehema Formation, a unit that interfingers with the Tuscan Formation and also contains interbeds of Nomlaki Tuff. Vertebrate fossils from the Tehama Formation just above the Nomlaki Tuff indicate a Late Pliocene (Blancan) age for the Tehama and Tuscan Formations and interbedded Nomlaki Tuff. Two fresh water diatom localities from Tuscan sections exposed east of Red Bluff yielded a variety of genera consistent with a Pliocene age (Lydon, 1969).

The Tuscan Formation tuff breccias formed as lahars or volcanic mudflows and had sources in the Cascades east of Seaman Gulch. Lydon (1969) has identified three major and at least four minor source areas of lahars of the Tuscan Formation. The major contributions came from the composite volcanoes of Mt. Yana, Mt. Maidu, and an area of indefinite structure that is located north of Latour Butte (Fig. 14). Some of the minor source areas include tuff breccia dikes south of Inskip Hill, a small area near Hatchet Mountain Pass and Campbell Mound.

Tertiary (?) Flow and Intrusive Rocks

Two varieties of Tertiary (?) flow rock crop out in the Seaman Gulch area; they are pyroxene andesite and basalt. The only Tertiary (?) intrusive rock present is a pyroxene andesite dike, perhaps a feeder to the compositionally equivalent flow.

Field Description

One small pyroxene andesite flow crops out in the Seaman Gulch area. This pyroxene andesite weathers to very shallow, blocky outcrops. The rock is medium light gray (N 6) in color, and generally aphanitic with sparse phenocrysts of magnetite psuedomorphs after amphibole. The pyroxene andesite flow rock appears to be very similar to fragments of andesite found in the lahars of the Tuscan Formation. Contact relationships with the Tuscan Formation and(or) the pre-Tertiary basement rocks were not exposed.

Basalt flows are present as discontinuous bodies as much as one-quarter square mile in area (0.65 km^2). They cap ridges in the northern part of the study area and unconformably overlie the Tuscan Formation and the pre-Tertiary basement. The contact between the basalt flows and the older rocks is steeply inclined where exposed. Distribution of the basalt flows suggests that they apparently filled stream valleys forming an erosional surface on the pre-Tertiary basement rocks. The basalts are medium gray (N 5) on weathered surfaces and grayish black (N 4) on fresh surfaces. Columnar jointing is common to this unit, with six-sided prismatic columns that are 10 to 12 inches (3.9 to 4.7 cm) in diameter. Thickness estimates for the basalt range from 40 to 75 feet (12.2 to 22.8 m).

Intrusive pyroxene andesite crops out in only one

locality; in the bottom of a small wash just east of a road cut that is located approximately 700 feet (213 m) N 30°E of diamond drill hole site 1 (Plate 2). This pyroxene andesite cuts the pre-Tertiary basement rocks and is dike-like in its occurrence. It is also located in close proximity to the pyroxene andesite flow to which it is mineralogically similar; thus, this dike may have served as a feeder to the flow. The intrusive pyroxene andesite is light gray (N 6) in color and is porphyritic. Phenocrysts consist of pyroxene and plagioclase feldspar that are set in an aphanitic groundmass.

Lithologic and Petrographic Descriptions

In thin section, the pyroxene andesite flow rock is microporphyritic and holocrystalline in texture. Microphenocrysts comprise 17.8 percent of the rock and consist of plagioclase feldspar, clinopyroxene, orthopyroxene, and magnetite psuedomorphs after amphibole. Groundmass textures are pilotaxitic and intergranular. The mineralogy of the groundmass consists of plagioclase feldspar, clinopyroxene, orthopyroxene, hornblende, Fe-Ti oxides and accessory apatite. Modal mineral percentages are listed in Table 5.

Microphenocrysts of plagioclase feldspar comprise 4.5 percent of the rock. They are subhedral, up to 1 mm in length, and calcic labradorite (An_{62}) in composition. Oscillatory zoning is common, whereas the patchy zoning as

Table 5. Modal Mineral Percentages for Tertiary (?) Flow and Intrusive Rocks

	Modal Analyses (Percent)		
	DP-30-78[1]	DP-92-78[2]	DP-117-78[3]
Phenocrysts:			
Plagioclase	4.5	23.8	23.4
Olivine	-	-	2.4
Clinopyroxene	7.1	7.2	3.4
Orthopyroxene	2.9	2.8	1.6
Magnetite Pseudomorphs after Amphibole	3.3	-	-
Groundmass:			
Plagioclase microlites	45.9	37.4	-
Clinopyroxene	7.1	6.4	TR[5]
Orthopyroxene	5.1	3.3	TR
Fe-Ti oxide	4.7	4.3	TR
Apatite	0.9	TR	TR
Hornblende	TR	-	-
Hyalopilitic Groundmass[4]	-	-	68.8
Alteration Products	18.2	14.7	-
Total	99.7	99.7	99.6

1) Pyroxene andesite flow; NE¼ NE¼ NE¼, Sec. 17.
2) Pyroxene andesite dike; NW¼ NW¼ NW¼, Sec. 16.
3) Basalt flow; SE¼ NE¼ SW¼, Sec. 8.
4) Hyalopilitic groundmass includes brown glass and plagioclase microlites.
5) Indicates present in trace amounts.

described by Vance is rarely observed. Zoning is normal and is characterized by calcic cores (An_{62}) and only slightly more sodic rims (An_{60} to An_{56}). Twinning is according to the albite and Carlsbad twin laws. Inclusions in these plagioclase feldspar microphenocrysts include apatite, clinopyroxene, orthopyroxene and Fe-Ti oxide.

Microphenocrysts of clinopyroxene (7.1 percent) are euhedral to subhedral in shape, 0.5 to 1.5 mm in diameter, and occasionally twinned. Optical properties, such as a very pale brown color, positive biaxial interference figure with an estimated 2V of approximately 50 to 60 degrees, and extinction angles of 36 to 42 degrees for longitudinal sections, indicate the clinopyroxene is probably augite.

Microphenocrysts of orthopyroxene comprise 2.9 percent of the rock. Prismatic crystals, 0.75 to 1.5 mm in length and subhedral in shape are most common. Their diagnostic optical properties consist of pale green to pink pleochroism, a negative biaxial interference figure with an invariably high 2V of greater than 70 degrees, and parallel extinction obtained from longitudinal sections. These optical features indicate that the orthopyroxene is hypersthene.

Magnetite forms complete psuedomorphs after phenocrysts of amphibole (3.3 percent). Some of the magnetite crystals have been partially to wholly oxidized to hematite.

The groundmass of this pyroxene andesite is composed of subhedral laths of plagioclase feldspar (45.9 percent) that are in subparallel alignment, less than 0.5 mm in length, and labradorite (An_{58}) in composition. Clinopyroxene (7.1 percent) and orthopyroxene (5.1 percent) in the groundmass are both less than 0.3 mm in diameter, subhedral to anhedral in shape, and display the optical properties of their respective microphenocrystic counterparts. The Fe-Ti oxide found in the groundmass is very uniform in size (0.3 mm), euhedral to subhedral, and often have thin rims of hematite. Apatite is present in the groundmass as small prismatic crystals, and trace amounts of subhedral hornblende are also present.

Alteration products of the primary minerals include hematite after magnetite, a clay mineral (probably smectite) after plagioclase feldspar, and an optically unidentifiable mineral that is colorless, has low relief and birefringence, and is interstitial to the major groundmass minerals. This mineral is probably alkali-rich feldspar that crystallized from a residual or deuteric liquid in the magma, or a devitrification product of glass that may have been either cristobalite or an alkali-rich feldspar.

The basalt is porphyritic and hyalocrystalline in texture. Phenocrysts include plagioclase feldspar, olivine, clinopyroxene and orthopyroxene. The texture of the groundmass is hyalopilitic. Brown glass, plagioclase

feldspar microlites, with subordinate Fe-Ti oxide and pyroxene are the principal constituents of the groundmass.

Phenocrysts of plagioclase feldspar (23.4 percent) are subhedral to euhedral in shape, as large as 2 mm, and bytownite (An_{71}) in composition. Oscillatory zoning in the plagioclase feldspar commonly envelopes an unzoned core that may have patchy extinction.

Anhedral phenocrysts of olivine (2.4 percent) are 0.4 to 2.0 mm in length, invariably corroded by the groundmass, and frequently rimmed by magnetite.

Clinopyroxene (3.4 percent) is the dominant mafic mineral of the basalt. It is present as phenocrysts that are anhedral to subhedral, range from 0.7 to 1.7 mm in length, and corroded by the groundmass. As their optimal properties are similar to those found in the pyroxene andesite flow, they are probably augitic in composition.

Prismatic phenocrysts of orthopyroxene (1.6 percent) are anhedral to subhedral in shape, and 0.7 to 1.25 mm in length. They commonly replace olivine, and in turn, are corroded by the groundmass. Optical properties indicate the orthopyroxene is hypersthene.

Intrusive pyroxene andesite is mineralogically very similar to the pyroxene andesite flow rock. The main difference between the two is textural; the intrusive rock is markedly porphyritic. Phenocrysts comprise 33.8 percent of the rock and include plagioclase feldspar, clinopyroxene and orthopyroxene (Fig. 16). The groundmass of the

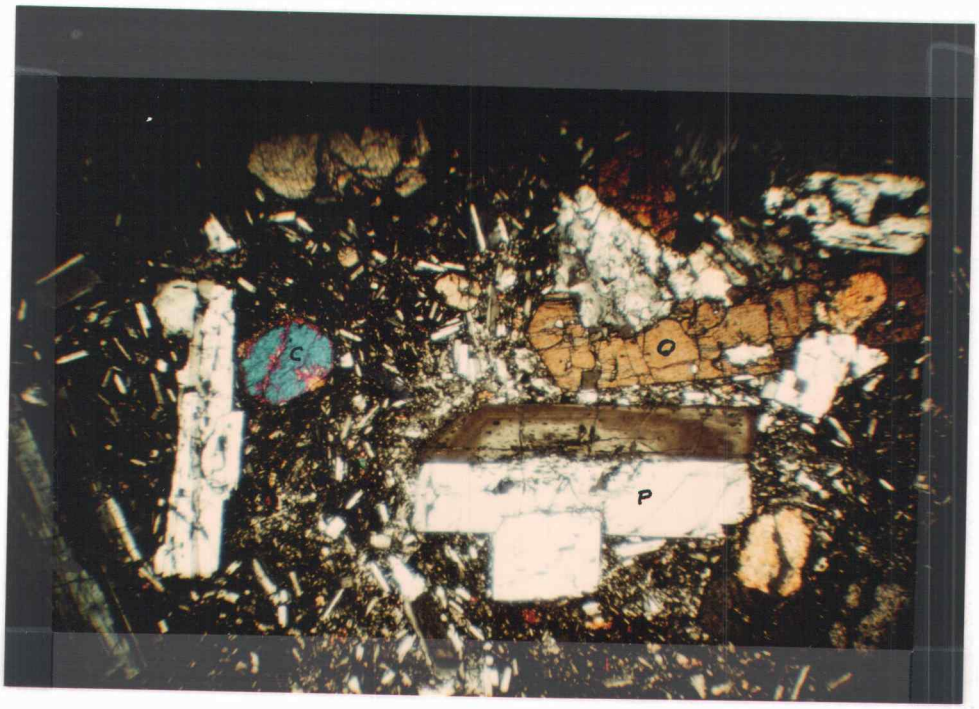

Figure 16. Photomicrograph of the pyroxene andesite dike from the NW¼, NW¼, NW¼, Section 16. Phenocrysts of plagioclase feldspar (P), orthopyroxene (O) and clinopyroxene (C). Field of view 4.5 mm (crossed nicols).

intrusive pyroxene andesite is mineralogically identical to its flow counterpart, and is texturally intergranular. Hornblende was not identified in the intrusive pyroxene andesite. Modal mineral percentages are listed in Table 5. Phenocrysts of plagioclase feldspar (23.8 percent) are calcic labradorite (An_{65}) in composition and slightly more calcic than their pyroxene andesite flow counterparts.

Clinopyroxene and orthopyroxene are identified optically as augite and hypersthene, respectively. Inclusions of clinopyroxene, Fe-Ti oxide, and rarely plagioclase feldspar are sometimes found in the phenocrysts of orthopyroxene.

The intergranular groundmass consists chiefly of randomly oriented subhedral to anhedral laths of plagioclase feldspar (An_{45}) with interstitial euhedra and subhedra of clinopyroxene, orthopyroxene and Fe-Ti oxide.

Chemical Composition

Major oxide and CIPW normative analyses for the pyroxene andesite flow (DP-30-78), the average andesite of LeMaitre (1976), and the average calcic andesite of McBirney (1969) are listed in Table 6 for comparison. Chemical analysis of pyroxene andesite showsf minor enrichments of SiO_2, Al_2O_3, MgO and CaO and depletions of TiO_2, total FeO, and K_2O compared to the average andesite of LeMaitre (1976). The relatively high CaO and low K_2O contents of this pyroxene andesite are compositional

Table 6. Major Oxide and CIPW Normative Values for Pyroxene Andesite Flow Rock (Sample # DP-30-78)

	Major Oxide Analysis (Percent)		
	1	2	3
SiO_2	60.74	57.94	58.68
TiO_2	0.58	0.87	0.81
Al_2O_3	17.72	17.02	17.29
FeO*	6.01	7.31	6.93
MnO	0.11	0.14	0.12
MgO	4.43	3.33	3.14
CaO	7.45	6.79	7.13
Na_2O	3.39	3.48	3.24
K_2O	0.83	1.62	1.27
P_2O_5	0.14	0.21	0.17
Total	101.39	98.71	98.78

	CIPW Normative Values (Percent)		
Qz	14.9	12.4	14.2
Or	4.9	9.6	7.7
Ab	28.4	29.4	29.7
An	30.4	26.0	29.5
Hy	12.8	9.5	9.9
Di	4.3	4.8	4.4
Mt	3.0	4.7	3.2
Il	1.1	1.7	1.2
Ap	0.3	0.5	0.4

1) DP-30-78 2) Average Andesite (LeMaitre, 1976)
3) Average calcic andesite (McBirney, 1969) 4) Total iron

effects that might be expected of an andesite having calcic parentage.

Age and Origin

The Tertiary (?) flow and intrusive rocks have not been dated radiometrically. However, a lower limit can be placed on the age of these rocks. In the Seaman Gulch area, the flow rocks unconformably overlie the Tuscan Formation which has previously been described as being Late Pliocene in age. Lydon (1969) described thick, but areally restricted pyroxene andesite flows (comprising part of the Mt. Yana composite volcano) between and above tuff breccia layers that are continuous with the main part of the Tuscan Formation. Petrographic descriptions of the Mt. Yana pyroxene andesite flows by Lydon (1969) are similar to those for the pyroxene andesite flow described in this investigation. If the pyroxene andesite flow described in the Seaman Gulch area is genetically related to the Mt. Yana flows, it also may be of Late Pliocene age. Albers and Robertson (1961) have suggested a Late Pliocene or Early Pleistocene age for basalt flows in the East Shasta district.

The dike of pyroxene andesite probably served as a feeder to the pyroxene andesite flow. The close proximity and mineralogical similarity of these two pyroxene andesites support this conclusion.

Quaternary Deposits

Unconsolidated deposits of Quaternary age post-date all other rocks in the Seaman Gulch area. The unconsolidated deposits are present as alluvium and colluvium. Alluvium fills portions of the major drainage in the Seaman Gulch area. Locally, it is present in mappable accumulations along some of the small tributaries of Seaman Gulch. These deposits formed by weathering and transport of all lithologies previously described in this investigation. Colluvium forms a veneer on many of the hill slopes and effectively obscures the bedrock in these areas.

METAMORPHISM

All of the pre-Tertiary basement rocks of the Seaman Gulch area have undergone some type of alteration since their deposition. Mafic pyroclastic rocks of the Dekkas Andesite have been converted in part to chlorite schist. Their secondary mineral assemblages contain some or all of the following minerals: chlorite, actinolite, albite, calcite, quartz, sphene, epidote, and white mica. In addition, pumpellyite, prehnite, stilpnomelane, and clinozosite are reported to be present by Albers and Robertson (1961). Silicic volcanics of the Bully Hill Rhyolite are composed of secondary mineral assemblages that contain quartz, white mica, clays, chlorite, albite, and calcite. Thus, these secondary minerals and (or) assemblages are properly relegated to the prehnite-pumpellyite facies and lower greenschist facies of regional metamorphism, ocean floor metamorphism, and geothermal metamorphism (propylitic assemblage).

The products of geothermal metamorphism are in intimate temporal and spatial association with volcanogenic sulfide mineralization. Minerals, in addition to the sulfides produced by this geothermal activity, are quartz, calcite, epidote, chlorite, white mica, anhydrite, Fe-Ti oxides, sphene, and clay minerals.

Because of the similarity in secondary mineral assemblages produced by the processes of regional metamorphism, ocean floor metamorphism, and geothermal

metamorphism, it is very difficult to ascertain which process(es) were responsible for the secondary minerals, with the exception of those associated with volcanogenic sulfide mineralization. Relict textures are generally well-preserved in these metavolcanics. Textures produced by deformation are preserved locally and are as follows: foliation; dimensional preferred orientation of fragments in chlorite schist of the Dekkas Andesite and in metadacitic lithic lapilli tuff of the Bully Hill Rhyolite; undulose extinction and strain lamellae in quartz; and pressure fringes composed of ribbon quartz surrounding pyrite. Volcanogenic mineralization and related geothermal (hydrothermal) metamorphism is of Late Permian age (see chapter on Economic Geology), whereas folding and regional metamorphism in the Seaman Gulch area were produced by deformation that is considered to be of Late Jurassic age in association with the Nevadan Orogeny (Albers and Robertson, 1961). However, it should be noted that a Middle Jurassic age (165 - 170 m.y.) has been assigned to much of Mesozoic deformation in lithotectonic terranes that lay west of the eastern Klamath belt in the Klamath Mountains (e.g. Fahan and Wright, 1983). Silberling and Jones (1982) noted that evidence of the Sonoma Orogeny (Late Permian - Early Triassic) is not recorded in rocks of the East Shasta District. Thus, it is proposed that the secondary mineral assemblages in the Seaman Gulch area formed in response to sub-sea floor geothermal activity

that was active during the development of the Dekkas Andesite - Bully Hill Rhyolite volcanic pile. The effects of subsequent deformation on the rocks of the Seaman Gulch area are not appreciable on the basis of the limited exposures available for examination.

STRUCTURE

The overall lack of exposures and marker units in pre-Tertiary rocks of the Seaman Gulch area rendered the mapping of structural features difficult. Faults and folds are the major structural features found in the area; although joints, foliation, and schistosity are also present.

Faults

Faults are probably present throughout the Seaman Gulch area, but they are not easily mapped because of the overall poor exposure. A high density of faults and(or) shear zones was found in drill core, but these structures could not be projected to the surface with confidence. The new faults mapped in the area strike either N. 50° - 60° E. or N. 20° - 45° W. and the dips are all steep (greater than 60°). In addition, faults served as conduits for the hydrothermal solutions that moved through the Seaman Gulch area as evidenced by the preferred distribution of sulfide minerals and associated hydrothermally altered rocks in and adjacent to these structures.

Folds

Folds are largely inferred from map relationships at the north end of Seaman Gulch and from the cross-section constructed through the area (Plate 1). Bedding features in the Dekkas Andesite and Bully Hill Rhyolite are not

readily discernible and thus, if present, are inferred to be similar in attitude to that observed in beds of shale that overlie these metavolcanic units. Fold axes in the shale strike approximately N 20° W. and plunge to the northwest. The inferred orientation of these fold axes differs markedly from those mapped in the Seaman Gulch area by Albers and Robertson (1961) who inferred the traces of fold axes to be from about N. 60° - 80° W.

Joints, Foliation, and Schistosity

Joints and a weak foliation are pervasively found throughout the pre-Tertiary rocks in the Seaman Gulch area, whereas well-developed schistosity is only locally present. Joints are best developed in the intrusive and(or) flow rocks of porphyritic metadacite, metabasaltic andesite, and altered intrusive basalt where they tend to be chiefly random in their orientation, although subordinate amounts of sheeted joints also are found. In addition, joints are erratically present in the metadacitic pyroclastic rocks of the Bully Hill Rhyolite and shales of the Pit Formation. In contrast, a weakly developed foliation is ubiquitous to the metadacitic pyroclastic rocks. This foliation strikes from N. 38°W. to N. 82° E. and dips are steep to the northeast or southwest. It is manifest by the preferred orientation of chiefly smectite and subordinate amounts of white mica. Attempts to relate the foliation to either faults or folds were difficult to impossible because of the

poor exposures found in the Seaman Gulch area.

Schistose rocks are found at two locations. Chlorite schist is present at the north end of Seaman Gulch, as previously described, in rocks that were originally basaltic tuff or basaltic tuff breccia of the Dekkas Andesite. The schistosity strikes from N. 60° - 72° W. and dips steeply to the northeast and southwest, and thus, does not parallel the trend of the fold axes depicted on Plate 1. Hence, this foliation may have formed during an episode of deformation other than that which generated the folds, although any speculation on the temporal relationship between these two structural events is limited by the lack of outcrop. Schistosity also is found locally developed in metadacitic pyroclastic rocks of the Bully Hill Rhyolite. These schistose pyroclastics have been intensely altered to an assemblage of chiefly smectite, quartz, and subordinate which mica and they are spatially coincident with a fault zone that parallels in part the northern contact of the intrusive basalt. The strike of this schistosity ranges from N. 20° - 38° W. and mimics those defined by the traces of nearby faults. In addition, lapilli-size fragments show a preferred orientation in this schist. The long axes of these fragments are oriented in the plane of schistosity. Thus, the spatial coincidence of intense alteration and schistosity with preferred orientation of fragments in the pyroclastics with faults suggests that hydrothermal activity and structural activity were largely contemporaneous.

ECONOMIC GEOLOGY

Mineralization in the East Shasta District has been described as being volcanogenic in origin and syngenetic with respect to the enclosing rocks (Anderson, 1969; Hutchinson, 1973; Ohmoto, 1978). Two types of sulfide occurrences are present; stratiform massive sulfide lenses, and(or) stringer veinlets and disseminations of sulfides in metadacitic rocks underlying the stratiform occurrences. The massive sulfide lenses are composed of banded sphalerite-pyrite-chalcopyrite-galena±tetrahedrite± bornite in a fine-grained baritic matrix. These massive sulfide lenses are found at the Pit Formation - Bully Hill Rhyolite contact at the Afterthought Mine (Albers and Robertson, 1961; Fredricks, 1980) in the southeastern portion of the district, and at three closely-spaced horizons near the top of the Bully Hill Rhyolite and including the Pit - Bully Hill contact at the Bully Hill and Rising star mines in the center of the district (Gustin and Eastoe, 1986). Stock-work veinlets and disseminations of barite±sulfides (pyrite, chalcopyrite, and sphalerite)±quartz and(or) carbonate are present in the immediate footwall of massive sulfide lenses and are characteristic of each horizon and occurrence. This footwall mineralization is, according to Albers and Robertson (1961) accompanied by hydrothermal alteration that consists chiefly of quartz, sericite, and minor amounts of chlorite and clays, and veinlets of

carbonate, anhydrite and(or) barite. In general, detailed descriptions of footwall alteration are lacking.

Approximately 750 thousand tons of massive sulfide ore was mined from the East Shasta District during the interval from 1900 to 1928. Typical assays of ore from the massive sulfide deposits were as follows: 15 to 20 percent zinc, 3 percent copper, 0 to 2 percent lead, 5 ounces silver per ton, and 0.03 ounce gold per ton. Virtually all of the massive sulfide ore came from three mines: the Bully Hill; Rising Star; and Afterthought. Production figures for the East Shasta Mining District are listed in Table 7. The recorded ore produced from this district would be approximately 115 million dollars at 1987 metal prices.

Activity in the East Shasta District commenced with the discovery of placer gold in the early 1850's. The extraction of precious metals from oxidized massive sulfide ore (gossan) followed the placer mining until the turn of the century, at which time the activity in the district shifted to the mining of the massive sulfide ore itself. Emphasis was placed on copper recovery from 1900 to 1920 and zinc recovery from 1921 to 1928. The Afterthought and Bully Hill mines were reopened briefly from 1949 to 1953. New orebodies were discovered during this period, but no ore was produced (Albers and Robertson, 1961). Exploration activity has been sporadic since 1953. The high grades of metals contained in these massive sulfide ores make them attractive exploration targets. From 1976 to 1978, Duval

Table 7. Summary of Massive Sulfide Ore Produced from the East Shasta District, 1900-1952. (Albers and Robertson, 1961.)

MINE	TONS MINED	COPPER (lbs)	ZINC (lbs)	LEAD (lbs)	SILVER (oz)	GOLD (oz)
AFERTHOUGHT	166,424	10,730,580	23,635,840	1,738,300	923,653	4,992
BULLY HILL RISING STAR	597,857	48,788,451	25,113,105	----	2,215,270	38,224
OTHER MINES	419	4,600	23,560	----	---	1
TOTAL	746,700	59,523,631	48,772,505	1,738,300	3,138,923	44,217

Corporation investigated an anomalous base metal-bearing gossan located south of Seaman Gulch in the NE¼, NE¼, NE¼, Sec. 17, T. 33 N., R. 2 W. This gossan was previously investigated by an unknown prospector(s) as evidenced by the presence of a thirty foot shaft, a collapsed adit, and several prospect pits. Methods employed by Duval Corporation during their investigation were reconnaissance geologic mapping, geochemical and geophysical surveys, and diamond drilling. Preliminary geologic maps, drill logs, and drill core were made available by Duval Corporation for use during this investigation. In addition, detailed geologic mapping (1:1200) and logging of 1500 aggregate feet of drill core at 1 inch = 10 feet were completed by the author.

Mineralization

Mineralization in the vicinity of Seaman Gulch that was examined during this investigation consists of sulfides containing iron, copper, zinc, lead and silver. These base and precious metal-bearing sulfides occur as disseminations, stringer veinlets, massive pods and irregular networks around pyroclastic fragments.

Host Rock

Silicic (metadacitic) volcanic rocks of the Bully Hill Rhyolite are host to the mineralization in the Seaman Gulch area, for which detailed descriptions of these rocks were

previously given (see chapter on Stratigraphic Units). All of the major sulfide occurrences are found in these silicic pyroclastic rocks, with minor amounts occurring as disseminations and veinlets in silicic intrusive rocks.

Mineralogy

The principal hypogene sulfide minerals identified in the Seaman Gulch area are pyrite, sphalerite, chalcopyrite, and tetrahedrite-tennantite. Galena was identified only microscopically. Some of these sulfides on the basis of assay values contain appreciable amounts of silver and trace amounts of gold. Examination of the mineralized samples in polished sections indicates that the majority of the sulfides are finely crystalline and intimately intergrown. Gangue minerals include quartz, calcite, and anhydrite (gypsum). Trace amounts of supergene "sooty" chalcocite are found as thin coatings on some of the sulfides in drill core.

Sulfide Minerals

Pyrite is ubiquitous and commonly the only sulfide mineral present; or when associated with other sulfide minerals it is by far the most abundant. Pyrite was deposited throughout the entire period of sulfide deposition. Early pyrite is frequently corroded and erratically replaced. The most common occurrence of pyrite is as subhedral to euhedral crystals up to 2 mm in diameter.

Sphalerite is the next most abundant sulfide present. It is one of the principal constituents of some of the massive pod and polymetallic stringer veinlet forms of mineralization. In such occurrences, it is intimately intergrown with chalcopyrite, pyrite, tetrahedrite-tennantite, and galena. Sphalerite is less commonly found as disseminations and is erratically distributed throughout the network mineralization. Disseminated and network occurrences of sphalerite are commonly corroded and replaced by pyrite; although subhedral crystals are sometimes present. The color of sphalerite crystals observed under transmitted light varies from light reddish brown to dark brown, and occasionally red. The color variations are a function of iron substituting for zinc in the dark brown crystals and abundant inclusions of tetrahedrite-tennantite in the red crystals. Some crystals contain light reddish brown cores with clear margins (Fig. 17). The clear margin may be the result of hydrothermal leaching or etching followed by the regrowth of colorless sphalerite that is often accompanied by fine inclusions of chalcopyrite.

Chalcopyrite is the third most abundant sulfide mineral present. It fills interstices and forms rims around corroded crystals of pyrite in the stringer veinlets, and is intimately intergrown with sphalerite, pyrite, tetrahedrite-tennantite, and galena in the massive pods. Veinlets of chalcopyrite $\pm$ anhydrite cut the massive pod occurrences, which clearly indicates that some of the

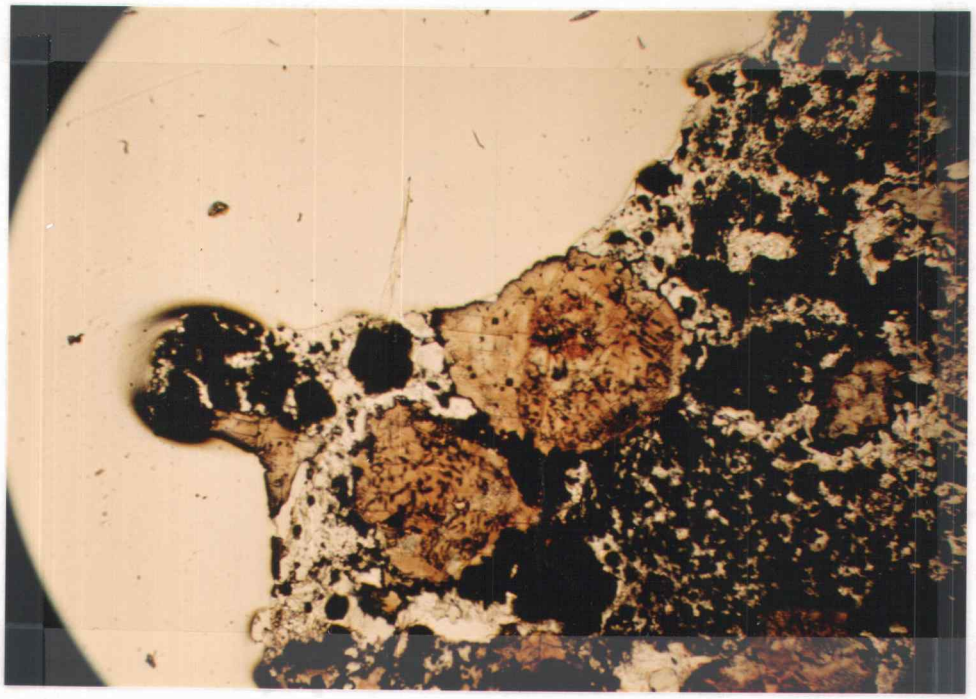

Figure 17. Photomicrograph of sphalerite with reddish brown cores and clear margins. The black mineral is pyrite and it is replacing sphalerite along its margins. Field of view is 2.0 mm (10x - plane light).

chalcopyrite is later than the bulk of the sulfide mineralization.

A tetrahedrite-tennantite group mineral occurs as intergrowths with chalcopyrite, pyrite, sphalerite, and galena in the massive pods and with sphalerite, chalcopyrite, and pyrite is stringer veinlets. Inclusions of tetrahedrite-tennantite are found in sphalerite where their distribution is crystallographically controlled. In addition, tetrahedrite-tennantite is also found as a minor component intergrown with chalcopyrite in late veinlets. This sulfosalt is believed to be the major source of silver in the ore-bearing mineral assemblage.

Galena is a rare and fine-grained constituent of the sulfides and was not observed megascopically. It is intimately associated with the copper-bearing minerals, chalcopyrite and tetrahedrite-tennantite, and less commonly with sphalerite. Some of the galena may be argentiferous.

The distribution of precious metals is very erratic. An examination of assay values indicates that high values of silver are generally associated with high values of zinc; and less commonly with high values of copper and(or) lead. These associations can be explained by examining the general chemical formula for tetrahedrite and tennantite are the antimony (Sb) - and arsenic (As)-rich end members, respectively. Copper (Cu) is always predominant, but considerable substitution takes place, most commonly by iron (Fe) and zinc (Zn), and less commonly by silver (Ag),

lead (Pb) and mercury (Hg) according to Palache, Berman, and Frondel (1944). Thus, substitutions of silver in the tetrahedrite-tennantite crystal lattice alone may explain many of the assay results obtained as many mineral associations given by textural evidence previously cited, whereby tetrahedrite-tennantite is sometimes a major component of the polymetallic stringer veinlets and massive pods that contain varying amounts of sphalerite (ZnS) and chalcopyrite ($CuFeS_2$). Gold values are generally low and its mode of occurrence has not been identified.

Trace amounts of supergene "sooty" chalcocite were found to coat massive sulfides at a depth of 176 feet in Drill Hole 3. The chalcocite is preferentially deposited as a replacement coating (film) on chalcopyrite and pyrite.

Gangue Minerals

Quartz is the most abundant gangue mineral. It is found interstitial to sulfide minerals in the massive pod and stringer veinlet textural types of mineralization and frequently in association with carbonate and anhydrite (gypsum). Quartz may be the only gangue mineral present, as is the case in the massive pyrite intercept at 285 feet in Drill Hole 2. Abundant tiny fluid inclusions are found in many of the quartz crystals. These contain a ubiquitous gas phase (bubble) and at least two solid phases. Ribbon quartz is present in highly altered and mineralized pyroclastic rocks that behaved plastically in response to

the regional stress regime that was imposed upon them. This ribbon quartz, as previously discussed in the chapter on metamorphism, formed in pressure fringes around pyrite grains.

Carbonate is also an abundant gangue mineral. At least two carbonate minerals were observed in thin section. The most common variety is clear sparry calcite that exhibits a well-developed rhombohedral cleavage. The least common variety consists of very cloudy anhedral crystals that may be siderite. Carbonate is frequently associated with quartz and anhydrite (gypsum), and locally it may be the only gangue mineral present. Most of the carbonate is late and was deposited interstitially to much of the late pyrite. In addition, some of the carbonate may have replaced the earlier gangue minerals. A few sulfide crystals were found to have been broken and rotated with carbonate infilling the newly created interstices. Veins and veinlets of carbonate cut all stages of hydrothermal alteration and mineralization. Carbonate also cements the altered basalt breccia.

Anhydrite is recognized petrographically by its near rectangular cleavage, high relief, and high birefringence. It occurs interstitial to the sulfide minerals in the massive pod and polymetallic stringer veinlets, accompanies chalcopyrite in veinlets that cut the massive pods, and is found as late veinlets that cross-cut the massive pods.

Anhydrite has been largely hydrated to gypsum within the zone of oxidation.

Paragenesis

The paragenetic order of mineral deposition in the Seaman Gulch area is based on crosscutting relationships, replacement textures in vugs and veins, and determined from both megascopic and microscopic scales of observation. Because the individual samples portray but a single episode, or a few episodes, of mineral deposition, the paragenetic sequence presented in Figure 18 was, of necessity, constructed by correlating like minerals and assemblages of consistent temporal position within the zone of mineralization. The assumption, implicit in this method, treat contemporaneous but dissimilar mineral assemblages (i.e. spatial variations) as having been precipitated during different intervals. A crude vertical zonal distribution of sulfide minerals and(or) assemblages from the bottom to the top of the system is as follows: (1) disseminated and stringer pyrite; (2) disseminated and stringer pyrite±chalcopyrite; (3) disseminated and stringer pyrite±chalcopyrite±sphalerite; (4) network pyrite±sphalerite±chalcopyrite; and (5) disseminated, stringer, and massive pod pyrite-sphalerite-chalcopyrite-tetrahedrite-tennantite±galena. These zonal relationships are illustrated by the generalized cross-section given in Figure 19. The vertical distribution of the sulfides is the result of

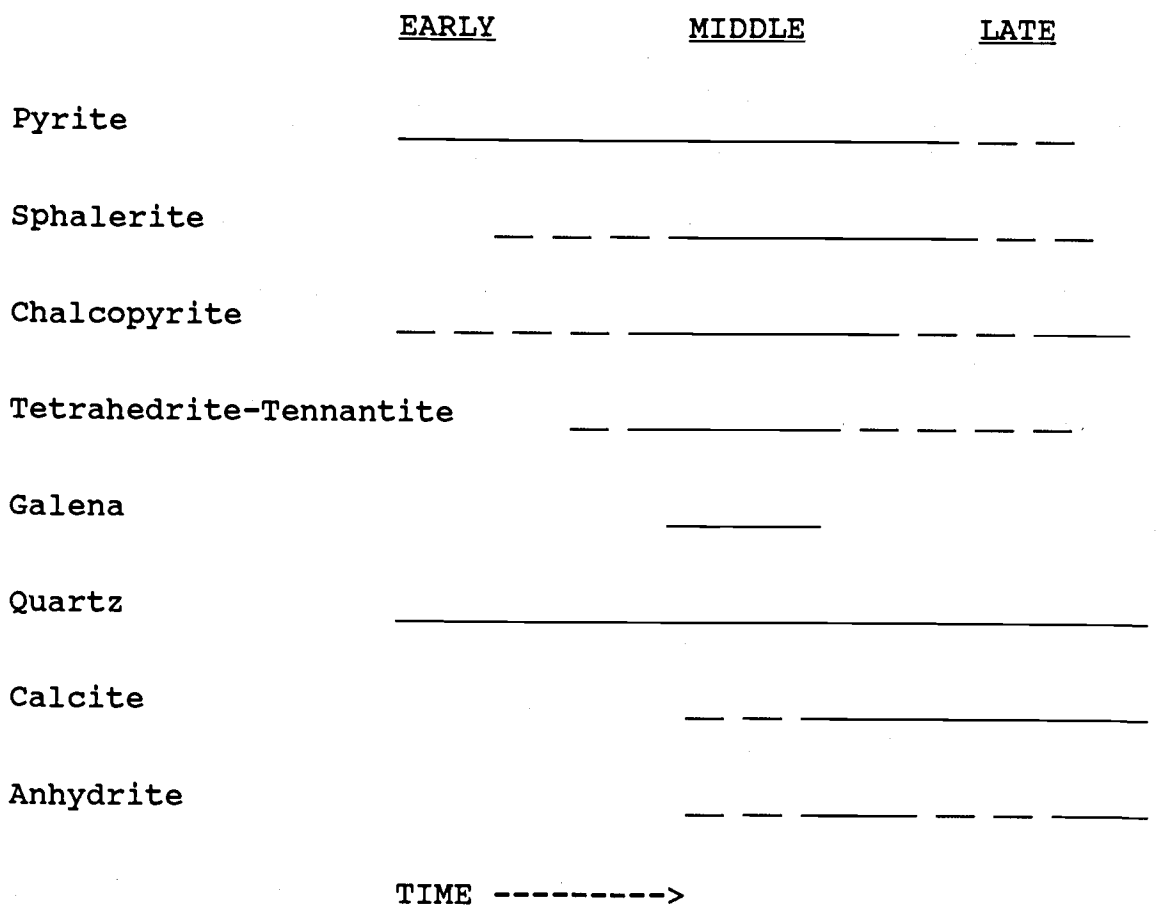

Figure 18. Relative paragenetic sequence for sulfide and gangue mineral deposition in the Seaman Gulch area.

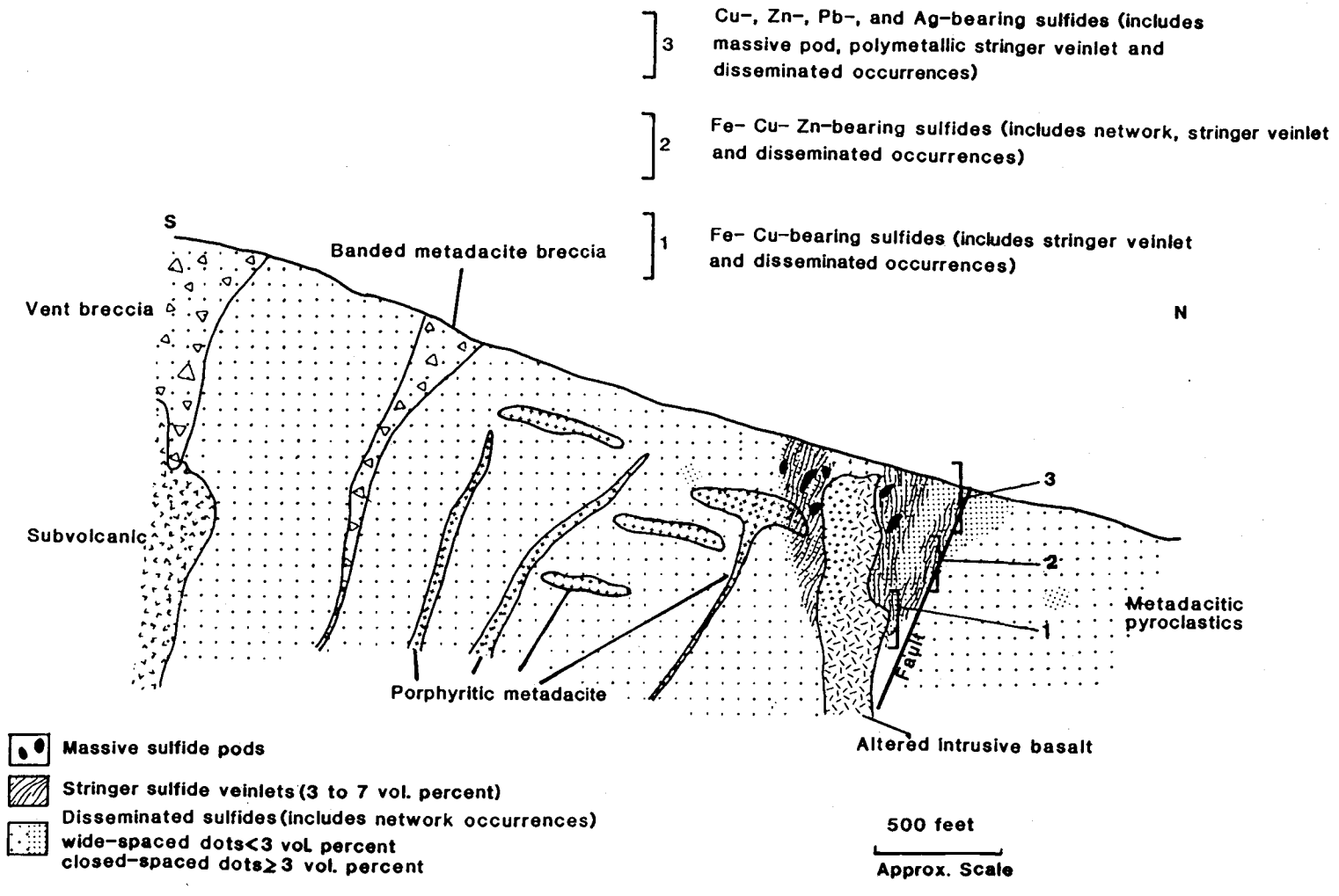

Figure 19. Idealized schematic cross section of geology adjacent to mineralization in the Seaman Gulch area that illustrates the spatial distribution of sulfide occurrences and vertical metal zonation.

differential precipitation from a cooling polymetallic hydrothermal solution as it ascended through the host rocks (see page 109).

In general, pyrite is the earliest sulfide mineral and formed throughout the entire period of sulfide deposition. Sphalerite and chalcopyrite appear next in both the deeper stringer and network types of mineralization. However, neither mineral was observed in association with the other in either of these occurrences. Thus, it is unclear if these two sulfides are contemporaneous, but spatially removed from each other. Pyrite, chalcopyrite, sphalerite, tetrahedrite-tennantite, and galena are intimately intergrown in the late-formed polymetallic stringer and massive pod occurrences. Chalcopyrite veinlets locally cut the massive pods. A slight change in composition of sphalerite with time is reflected in a color change from early dark brown and dark reddish-brown varieties that are commonly replaced by pyrite to late light reddish-brown and red varieties that frequently contain inclusions of tetrahedrite-tennantite or chalcopyrite.

Quartz is the earliest gangue mineral to have been deposited. It apparently was formed throughout the entire episode of mineralization. Nonetheless, its distribution is not ubiquitous. Anhydrite is relatively late. It is found in the interstices of some of the polymetallic massive pods. In addition, it may also be present with the late chalcopyrite veinlets, as well as localized in late

monomineralic veinlets that cut the entire massive pod assemblage.

Carbonate is the latest gangue mineral to have been deposited. It replaces earlier gangue minerals, infills voids between fragmented sulfide crystals, occurs as late veinlets cutting all other minerals, and the paragenetically earliest forms of carbonate are interstitial to sulfide and other gangue minerals.

Structural Characteristics

Controls that served to localize or channel the solutions from which sulfide minerals precipitated in the Seaman Gulch area are as follows: (1) intrusive - country rock contacts; (2) the highly permeable and porous pyroclastic rocks; (3) faults; and (4) fractured country rock.

The relationship of the surface distribution of the gossan to the contact of the altered intrusive basalt is the most striking structural control in the area. The arcuate outcrop pattern of the gossan closely mimics the contact of the altered basalt (see Plate 2). Drill core intercepts indicate that mineralization follows this contact zone in the subsurface. The intensity of mineralization along this zone suggests that this area was the principal conduit through which the ascending hydrothermal solutions passed. Two interrelated reasons are given as to why this zone was the focus of mineralization. These are

because: (1) the contact zone between altered intrusive basalt and silicic pyroclastic rocks produced a permeable zone that served to channel the ascending hydrothermal solutions; and(or) (2) much of the altered intrusive basalt along this contact zone, especially the southern portion, was brecciated by an explosive hydrothermal event. Brecciation of the adjacent silicic volcanic country rock was minimal, but much fracturing did occur. Hence, a permeable zone of brecciated and fractured rock provided structural channelways for the ascending hydrothermal solutions.

The initial porosity and permeability of the silicic pyroclastic rocks played an important role in channeling the ascending hydrothermal solutions. Network and less commonly stringer veinlet sulfide occurrences and their associated hydrothermal alteration products can readily be observed winding their way through and around the framework fragments in the silicic pyroclastic rocks. In addition, fault and fracture control of mineralization and alteration is found in the widespread distribution of structurally controlled vein, veinlet, stockwork and seam occurrences of the ore and gangue minerals.

Wall-Rock Alteration

Wall-rock alteration is pervasive throughout the pre-Tertiary country rocks in the Seaman Gulch area. As was previously discussed in the chapter on metamorphism, it is

often difficult to determine which processes are responsible for the changes in mineral assemblage; those attributed to geothermal (hydrothermal) alteration, or those related to diagenetic or low grade regional metamorphic phenomena.

Hydrothermal alteration is a type of hydrous metamorphism that involves recrystallization and reconstitution of a parent rock to new minerals as dictated by changes in chemistry, pressure, and temperature of the environment. Creasey (1959) pointed out that the minerals formed by hydrothermal alteration may be classified in the same manner as minerals formed by regional and contact metamorphic processes whereby the mineral assemblages formed with alteration reflect the temperature, pressure, chemical composition of the hydrothermal fluid, chemical and mineralogical composition of the parent rock, and time available for equilibration. Hydrothermal alteration takes place because a fluid, liquid, or gas has the capacity to transfer chemical constituents and heat; and typically involves large amounts of fluid traversing rocks through assorted plumbing systems. Reaction with the hydrothermal fluids causes changes in the chemical composition of the host rocks that in turn produce zonations of alteration minerals that reflect the extent and duration of the reactions between fluids and rock.

Alteration minerals identified in host rocks of the Seaman Gulch area include chlorite, quartz, white mica,

carbonate, anhydrite, epidote, and clay minerals. The chief alteration, silicification, propylitic alteration, argillic alteration (both hypogene and supergene), and carbonate alteration.

Chloritic Alteration

Pervasive chloritization is found in both silicic pyroclastic rocks and the altered intrusive basalt and basalt breccia. The chloritic assemblage of silicic pyroclastic rocks is characterized by the presence of appreciable amounts of chlorite (20 to 40 percent), ubiquitous pyrite, and subordinate amounts of quartz, white mica, sphene (leucoxene), anhydrite, chalcopyrite, and sphalerite. Chlorite chiefly replaces matrix material and corrodes and embays the edges of lithic fragments. Less commonly, the lithic fragments may be completely replaced by chlorite. Although sulfide mineralization (chiefly pyrite) is ubiquitous to the zone of chloritic alteration, it is suggested that the sulfides formed later than the chlorite on the basis of cross-cutting relationships. Chemical analysis of chloritically altered silicic pyroclastic rock (Table 8 and Fig. 20, Sample D) shows relative enrichment of MgO and total iron (as FeO), and corresponding depletion of SiO_2, CaO, Na_2O, K_2O, and Al_2O_3. Much of the increase in total iron can probably be attributed to the addition of pyrite to the rock.

Chloritic alteration of the altered intrusive basalt

Table 8. Chemical Analyses of Hydrothermally Altered Silicic (Metadacite) Volcanic Rocks from the Seaman Gulch Area

	Major Oxide Analyses (Percent)			
	A	B	C	D
SiO_2	63.4	68.8	74.3	54.1
TiO_2	0.4	0.5	0.5	0.4
Al_2O_3	12.8	13.8	12.2	11.6
MgO	2.0	1.4	0.3	8.1
FeO*	7.8	7.7	4.7	16.3
MnO	0.1	0.2	0.1	0.2
CaO	0.5	1.4	0.3	0.2
Na_2O	5.3	6.0	4.6	0.8
K_2O	0.2	0.1	0.9	0.3
P_2O_5	0.1	0.1	0.1	0.1
TOTAL	97.6	100.0	98.0	92.1

A) Metadacitic lapilli tuff from the outer propylitic zone.

B) Metadacite dike from the inner propylitic zone.

C) Metadacitic lapilli tuff from the quartz-white mica zone.

D) Metadacitic lapilli tuff from the zone of chloritic alteration.

*Total iron

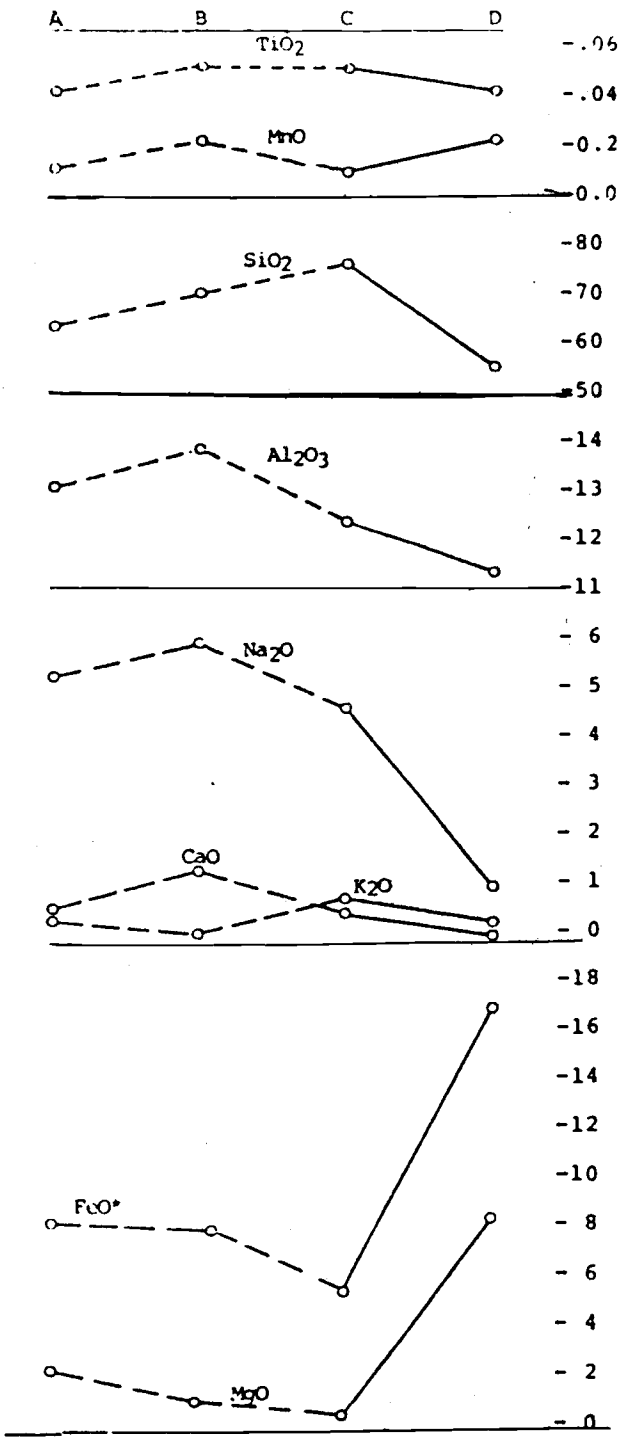

Figure 20. Chemical variations between zones of hydrothermal alteration. A - outer propylitic zone. B - inner propylitic zone. C - quartz-white mica zone. D - zone of chloritic alteration.

is not only characterized by appreciable amounts of chlorite, but also by subordinate amounts of calcite, quartz, sphene (leucoxene), and clay minerals. Chlorite chiefly replaces microphenocrysts and laths of plagioclase feldspar. Psuedomorphs of chlorite that completely replace the host feldspar are common. Microphenocrysts of clinopyroxene have been similarly altered to chlorite. Incipient replacement of clinopyroxene by chlorite is manifest by the presence of wispy aggregates along fractures, corroded crystal margins, cleavage traces, and twin planes. Elsewhere, but less commonly, complete replacement of the pyroxene by chlorite is sometimes observed. Ferromagnesian minerals of the groundmass may be completely replaced by chlorite. Two whole rock analyses of the altered intrusive basalt were listed in Table 4. The apparent chemical effects are high total iron (FeO*) and slight enrichment of Al_2O_3, and slight depletion of SiO_2, CaO, MgO and P_2O_5. However, relative changes in major oxide chemistry cannot be estimated for lack of an unaltered sample with which a comparison can be made.

Silicification

Silicification is a prominent type of alteration in the Seaman Gulch area. It is distinguished by abundant veinlets and stockworks of quartz, replacements by quartz of plagioclase feldspar in silicic pyroclastic and intrusive rocks, and in the altered basalt, anhedral

mosaics of quartz flooding the matrix and less commonly the framework fragments in silicic pyroclastic rocks, vug fillings, replacement by microcrystalline quartz in the groundmass or matrix of silicic volcanics, and thin secondary overgrowths of quartz along the margin of phenocrysts and crystal fragments of quartz.

Quartz-White Mica Alteration

Silicic pyroclastic rocks located in the N½, SW¼, Sec. 16 have been intensely altered to quartz, white mica (possibly sericite), and pyrite. Relict textures are visible, although replacement is complete. This quartz-white mica alteration assemblage has been extensively overprinted by a later argillic assemblage consisting of smectite (possibly Na-rich montmorillonite) and subordinate kaolinite that have replaced white mica and corroded quartz.

Chemical analysis of this alteration type (Table 8 and Fig. 20, Sample C) indicates relative enrichment of SiO_2 and K_2O and corresponding leaching of CaO and MgO. However, because of the extensive argillic overprinting and absence of density data, any relative chemical gains and losses must be treated with caution. SiO_2 and K_2O were probably added and Na_2O subtracted during recrystallization of the rock to a quartz-white mica assemblage. Weak leaching of SiO_2 and K_2O accompanied by Na_2O enrichment may have taken place during later argillic overprinting.

Propylitic Alteration

Propylitic alteration of silicic volcanic rocks is identified by the presence of chlorite, epidote, calcite, clay minerals, albite, quartz, Fe-Ti oxides and pyrite. Glomerocrysts and phenocrysts of plagioclase feldspar show partial to complete replacement by any one of or a combination of albite, epidote, calcite, and clay minerals. Psuedomorphous aggregates after ferromagnesian minerals (chiefly amphibole) consist of chlorite, Fe-Ti oxides, smectite, calcite, and pyrite. Propylitized rock can be divided into an inner propylitic zone (IPZ) and an outer propylitic zone (OPZ). The IPZ is characterized by relatively abundant epidote (up to 4.1 percent) and chlorite (up to 11.3 percent). In contrast, the OPZ is characterized by weak replacement of plagioclase feldspar cores by clay minerals and(or) calcite (up to 4.6 percent). Chlorite is weakly developed in the OPZ where it is restricted to the groundmass or matrix. Epidote is present in trace amounts. Chemical analyses of these propylitized rocks are listed in Table 8 (Samples A and B). The data suggest possible additions of Al_2O_3, Na_2O, and CaO with increasing intensity of propylitization.

Carbonate Alteration

Carbonate, chiefly calcite and possibly subordinate siderite, forms a late hydrothermal alteration type. A

well-developed carbonate halo is found along the contact zone of the altered intrusive basalt. Carbonate replaces all minerals in this basaltic host rock and cements the altered basalt breccia. Elsewhere, it forms veins and veinlets that cut all of the country rocks. Calcite is also found as a late gangue mineral associated with the sulfide mineralization.

Argillic Alteration

Both hypogene and supergene argillic alteration assemblages are found in the Seaman Gulch area. Pervasive strong argillic alteration that overprints the earlier quartz-white mica alteration was previously described. Other hypogene argillic alteration is ubiquitously found associated with late disseminations of pyrite±sphalerite in the silicic volcanic rocks. This alteration consists of small patches of abundant smectite with sulfides in what is otherwise a weakly altered rock of the outer propylitic zone.

Supergene argillization is widespread in the Seaman Gulch area. Details of its occurrence and distribution will be discussed in a later section concerning oxidation and supergene alteration.

Zonation

The hydrothermal alteration assemblages that have been previously described show a regular zonal distribution.

Each alteration type is dominated by a single mineral or mineral assemblage. The alteration mineral or assemblage characteristic of each alteration type may not be the dominant assemblage at the local scale. However, the dominant assemblage can be recognized readily when considered at a larger scale. The distribution of the zones of hydrothermal alteration are schematically illustrated in Figure 21. The altered intrusive basalt is the approximate center of hydrothermal activity and is strongly chloritized throughout. The surrounding silicic volcanic rocks exhibit a zone of chloritic alteration in the deeper portions of the system. This chlorite zone grades upward into a zone of quartz-white mica alteration, and laterally into the inner propylitic zone. The appearance of anhydrite is characteristic of the transition zone between the chlorite and quartz-white mica alteration zones. The quartz-white mica zones grade laterally into the inner propylitic zone also. The inner propylitic zone merges transitionally into the outer propylitic zone. Silicification is widespread but its distribution is difficult to ascertain because quartz is frequently a minor component of the other alteration assemblages and much of the formation of secondary quartz is recognized microscopically. Nevertheless, zones of quartz veinlets and(or) quartz flooding are found best-developed peripheral to the center of hydrothermal activity. Alteration overprinting is widespread and consists of two types and episodes; (1) carbonate alteration, and

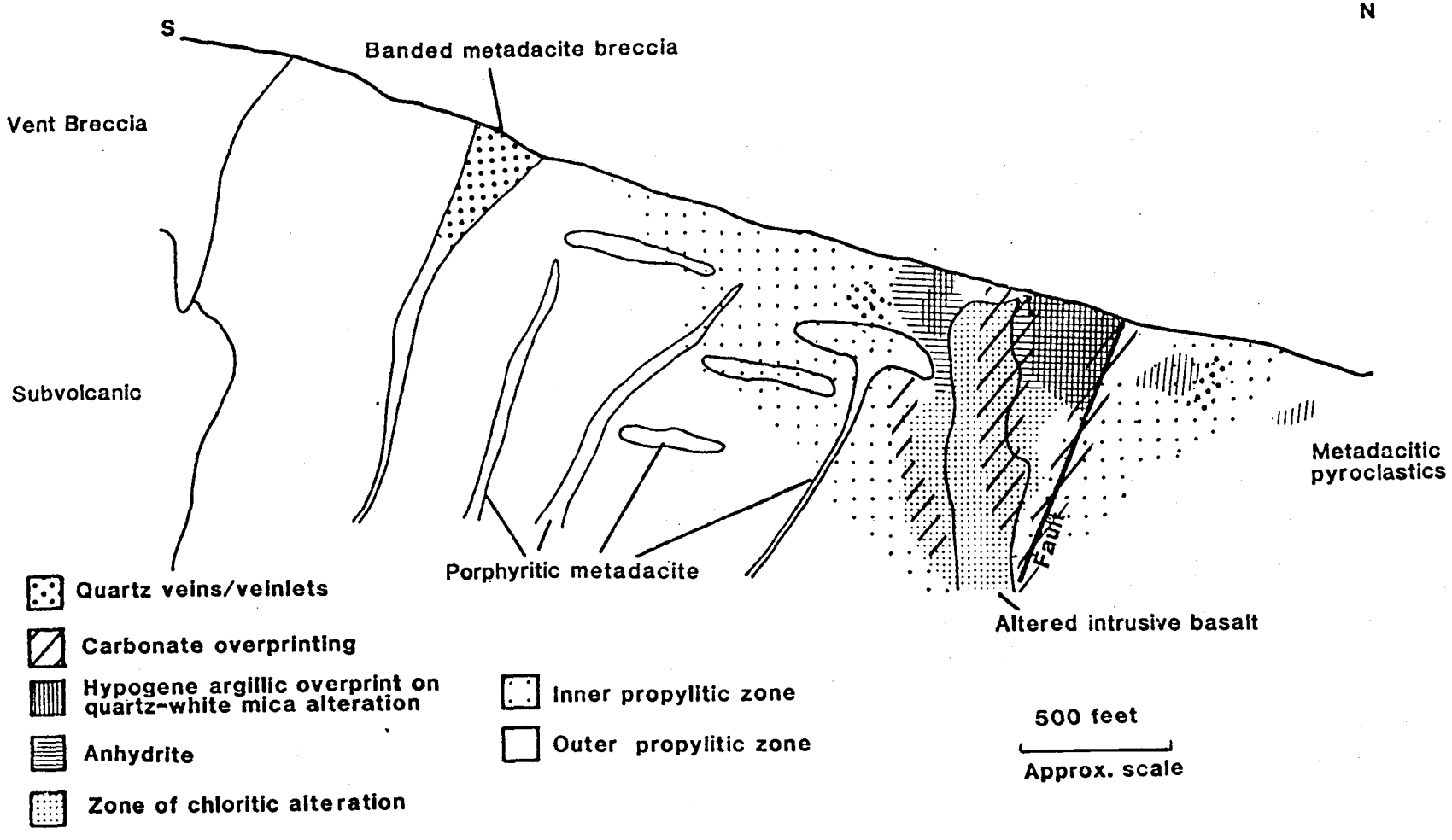

Figure 21. Idealized schematic cross section of geology adjacent to mineralization in the Seaman Gulch area that illustrates the distribution and overprinting of hydrothermal alteration.

(2) argillic alteration. A definitive age relationship was not directly observed, but the argillic alteration is believed to be the later of the two. Relatively late carbonate forms a halo that approximates the surface contact of the altered intrusive basalt. The amount of carbonate steadily increases from the central portion of this intrusion to its margins. The carbonate partially to totally replaces all minerals in the altered intrusive basalt, as well as being the only mineral that cements the altered basalt breccia. Strong argillic overprinting of the quartz-white mica zone has occurred. Similar, but erratcially distributed, argillic overprinting of the inner propylitic zone and outer propylitic zone is also found in intimate association with late disseminations of pyrite$\pm$ sphalerite.

Oxidation and Supergene Alteration

Gossan crops out in an arcuate pattern that approximately parallels the contact of the altered intrusive basalt (Fig. 22). The gossan is the oxidized equivalent of the mineralized silicic pyroclastic rocks. The primary textures found in the mineralized silicic pyroclastic rocks are closely mimicked by the gossan as evidenced by the presence of quartz and altered fragments of feldspar crystals, and altered lithic fragments that are set in a limonitic matrix. The total limonite component (a mixture consisting predominantly of goethite, some hematite, and subordinate jarosite) of the gossan varies from nearly

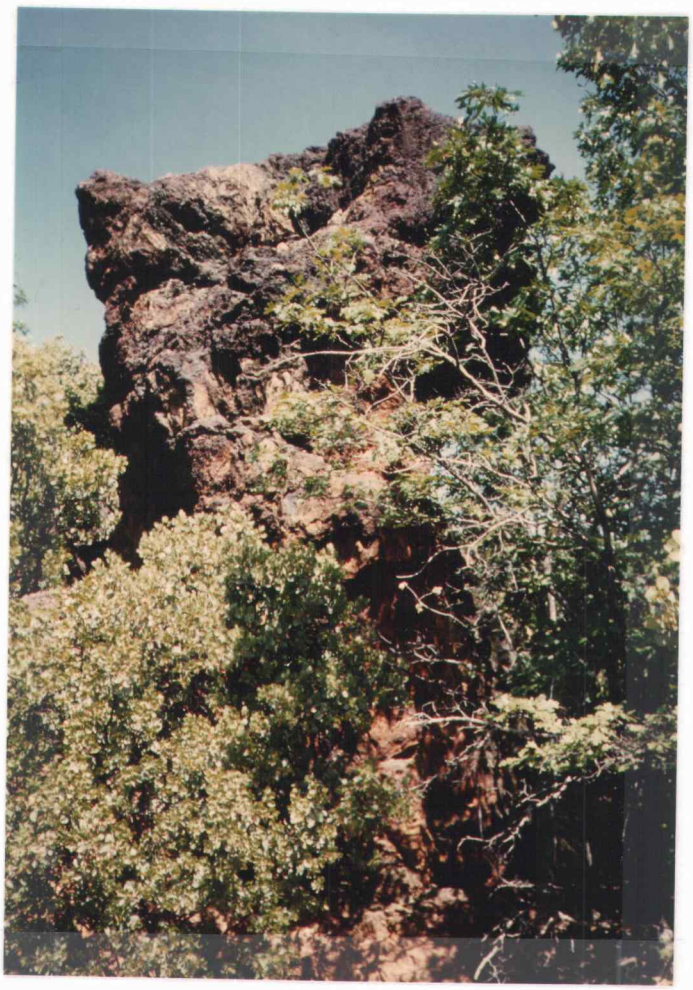

Figure 22. Outcrop of gossan formed from disseminated and stringer veinlet sulfide occurrences that are hosted by metadacitic lithic tuff breccia.

massive to small quantities of disseminated blebs. These variations reflect the percentage and textural occurrence of total sulfide originally present in the rock prior to oxidation. Two textural varieties of massive gossan are found; (1) the first consists entirely of a very finely-cellular sponge texture, and (2) the second consists of stockwork of limonitic jasper.

Blanchard (1966) has provided a detailed discussion regarding the formation of these textures which is summarized as follows. The finely-cellular sponge texture is the product of psuedomorphous replacement of sulfide by limonite which generally portrays a replica of the fracture or grain pattern of the sulfide undergoing decomposition. As more of the decomposing sulfide passes into solution, the open-spaces increases, until under favorable conditions a well-knit sponge develops. The formation of the stockwork of limonitic jasper after an alumino-silicate rock is a replacement process that proceeds by two separate though usually related stages: (1) kaolinization of the rock to "soap"; and (2) impregnation and replacement of the "soap" by silica plus ferric oxide hydrate (limonitic jasper). The term soap is used by Blanchard to distinguish a special type of supergene argillic alteration (kaolinite with or without smectite) from the more widespread kaolinized product derived from the general process of weathering. Soap occurs as localized, strongly bleached seams, nodules, or lenses of erratic distribution. It is distinguished by

virtue of its much whiter, bleached appearance, from the less altered enclosing rock, and its texture is not earthy; but, instead is characterized by smooth, curved surfaces that show evidence of frictional polish (slickensides). Because of the intense alteration and leaching involved, soap is virtually free from constituents other than those comprising minerals of the kaolinite and(or) montmorillonite groups. Such replacement occurs most often and in greatest volume where alumino-silicate rocks contain or are in close proximity to semi-massive to massive pyrite.

Oxidation of sulfides, chiefly pyrite, by oxygen in the presence of water yields sulfuric acid and ferrous sulfate. Hence, ground waters percolating through pyrite-rich country rock will react with the pyrite to produce acid solutions. These oxidizing acid solutions react with the country rocks to produce more stable mineral assemblages as may take place under hypogene conditions with strongly acid hydrothermal fluids. This type of supergene alteration is widespread in surface outcrops of the mineralized horizon throughout the Seaman Gulch area and the East Shasta District. Large, irregular areas of silicic volcanic rocks have been bleached and extensively altered to kaolinite, especially adjacent to the main gossan occurrence. Insoluble iron oxides (limonites) have precipitated along fractures in the surficial outcrops of these host rocks that have been altered by supergene processes.

Age of Mineralization

Mineralization in the East Shasta District consists of two types: stratiform massive sulfides; and disseminated and(or) stringer (stockwork) sulfides. The massive sulfide bodies of the East Shasta District have been described as being volcanogenic in origin and syngenetic with respect to the enclosing rocks (e.g. Hutchinson, 1973). Stringer and disseminated occurrences underlie the massive sulfide bodies and are epigenetic with respect to their host rocks, but they represent the subsurface conduits or the plumbing system through which hydrothermal fluids ascended before venting at the sea floor where precipitation of massive sulfide occurred (see chapter on Genesis of Mineralization). The massive sulfide deposits of the East Shasta District are chiefly found along the Pit Formation - Bully Hill Rhyolite contact and have been assigned a Late Permian age by Gustin and Eastoe (1986). Sulfide mineralization in the Seaman Gulch area occurs chiefly as disseminations and stringer veinlets that are composed of pyrite±chalcopyrite±sphalerite±tetrahedrite-tennantite. These sulfides are associated with hydrothermal alteration assemblages that are as follows: chloritic alteration, quartz-white mica alteration, silicification, argillic alteration, carbonate alteration, and propylitic alteration. Massive sulfide deposits were not found in the Seaman Gulch area, but the stringer and disseminated sulfide occurrences are interpreted to be contemporaneous with those underlying

massive sulfide bodies elsewhere in the East Shasta District because they are similar in composition and occurrences of sulfides associated with hydrothermal alteration, and of relative stratigraphic position (i.e. the upper part of the Bully Hill Rhyolite). Accordingly, the mineralization in the Seaman Gulch area must also be of a Late Permian age.

Genesis of Mineralization

Massive sulfide deposits in the East Shasta Mining District have been interpreted by Anderson (1969) as being volcanogenic in origin and placed in the volcanogenic classifications of Hutchinson (1973) and Ohmoto (1978). Sawkins (1976) listed the massive sulfide occurrences in the East Shasta District under the Kuroko-type subclass of submarine volcanogenic massive sulfide deposits. Similarities between massive sulfide deposits in the East Shasta District and Kuroko deposits are as follows: (1) deposits tend to occur as clusters of lenses; (2) both show a strong spatial correlation with silicic explosive volcanism; (3) both contain two types of ore, stratiform massive sulfides (syngenetic) and stringer vein and disseminated sulfide occurrences that cuts the footwall stratigraphy (epigenetic); (4) both contain anhydrite-gypsum ores; (5) both are capped by a layer of ferruginous chert-hematite; (6) both show compositional zoning relative to stratigraphy with zinc-lead increasing upward and copper decreasing upward; (7) massive sulfide lenses are underlain by alteration

minerals that enclose stringer and disseminated ores; and (8) the massive sulfide bodies contain similar sulfide suites composed of pyrite, sphalerite, chalcopyrite, galena, tetrahedrite, and bornite. The most noteable difference between massive sulfide deposits from these two districts is that post-ore alteration of hangingwall rocks, which can be directly related to mineralization in the Kuroko deposits has not been documented in the deposits found in the East Shasta District. Based on descriptions by Albers and Robertson (1961), the Bully Hill, Rising Star, and Afterthought mines have been equated with Kuroko-type deposits from their type-section area in the Kuroko District of northern Honshu, Japan (Table 9).

Mineralization and associated hydrothermal alteration assemblages present in the Seaman Gulch area are typical of those found in the footwall (stockwork or stringer zone) plumbing system of a Kuroko-type deposit. The sulfide occurrences and local geology bear similarities to both Type I and Type II Kuroko-type deposits described by Colley (1976) for similar occurrences in Fiji. The zonations of sulfide and hydrothermal alteration mineral assemblages are also very similar to those commonly found in Kuroko-type deposits. The intimate spatial relationships and zonations between sulfide and hydrothermal alteration mineral assemblages are schematically illustrated in Figures 19 and 21. The following relationships should be considered relevant when postulating the genesis of mineralization in

Table 9. Comparison Bewteen Kuroko-type Deposits in Japan and the East Shasta District

		JAPAN	EAST SHASTA DISTRICT
Regional Geology		Occur within Miocene 'Green Tuff' belt in slightly metamorphosed silicic volcanic rocks	Triassic (?) Bully Hill Rhyolite - weakly metamorphosed submarine silicic volcanic rocks
Position of mineralization in volcanic cycle		Waning stages	Waning stages
Associated silicic volcanic dome		Usually present	Probably present; more detailed mapping is required
Ore bodies		Massive lenses that are overlain by unmineralized rock and underlain by stockworks and alteration pipes	Similar to Japanese deposits
Distribution and location of ore bodies		Massive lenses tend to occur in clusters or districts related to centers of volcanic activity	Similar to Japanese deposits
Stratigraphic succession of ore and rock types in descending order:			
	Hangingwall:	Upper volcanic and sedimentary formation	Shale with intercalated tuff (Pit Formation)
(Tetsusekiei)	Ferruginous Quartz Zone	Hematite-quartz±pyrite	Quartz-hematite±pyrite, Albers and Robertson (1961) Probable stratigraphic position
	Barite Ore Zone	Composed of massive barite ore	Present at Bully Hill Mine (Albers and Robertson, 1961) and Afterthought Mine (?)
(Black) (Yellow)	Kuroko Ore Zone Oko Zone	Sphalerite-galena-barite Pyrite-chalcopyrite	Probable; Albers and Robertson (1961) describe three main ore types at the Bully Hill Mine. They are as follows: 1) banded sphalerite-pyrite-chalcopyrite-galena (black ore); 2) pyrite-chalcopyrite±sphalerite (yellow ore); and 3) chalcopyrite-pyrite±sphalerite (Keiko?). The boundary between the three types of ore may be sharp or gradational.
	Sekkoko Zone	Anhydrite-gypsum-pyrite ore	Present at Rising Star Mine (Albers and Robertson, 1961)
(Siliceous)	Keiko Zone	Chalcopyrite-pyrite±sphalerite±galena, siliceous, disseminated and/(or) stockwork ore	Similar; Bully Hill and Afterthought Mines (Albers and Robertson, 1961); Seaman Gulch area (this study)
	Footwall	Silicified rhyolite and pyroclastic rocks, disseminated and veined by sulfides	Hydrothermally altered silicic volcanic rocks with disseminations, veinlets, and massive pods of sulfides
Alteration		Generally pipe-like in shape with a silicified (±sericite±chlorite) core overlain by argillized rock (sericite-chlorite facies within the massive ore body itself and just above it and montmorillonite-zeolite facies above the ore body). The chemical variations involved in alteration of the footwall volcanic rocks of felsic composition are the relative depletion of Na_2O and CaO and the increase of H_2O and S.	Similar; however chlorite-white mica (sericite?) are relatively more abundant and silicification less abundant in the footwall zone (this study and the Afterthought Mine, Albers and Robertson (1961). Argillization (post-smectite ore) is recognized in the district; however, zeolites are not found and this is probably due to the grade of regional metamorphism (lower greenschist facies). Similar chemical variations involved in the alteration of footwall silicic volcanic rocks are found (this study). The increase in sulfur in the footwall volcanic rocks is inferred from the abundant sulfide minerals that are present.

the Seaman Gulch area: (1) the regional geologic setting of massive sulfide deposits in the East Shasta District as a whole (including the Seaman Gulch area) is intimately associated with the waning stages of silicic volcanism that occurred in an island arc environment; (2) a crude vertical metal zonation is present that is consistent with that characteristic of Kuroko-type deposits, although a syngenetic massive body overlying the epigenetic stockwork or stringer zone is absent; and (3) the relative chronological sequence of events that occurred during mineralization. This sequence of events is as follows: (1) a relatively early pre-mineralization episode that involved chloritization and silicification of the silicic volcanic rocks and intrusive basalt, accompanied by gradational lateral development of the inner propylitic zone and the outer propylitic zone; (2) brecciation of the altered intrusive basalt; (3) hydrothermal deposition of sulfides and sulfates in silicic volcanic rocks; (4) sealing of the hydrothermal conduits (fractures) by calcite and quartz; (5) intense argillic overprinting of the quartz-white mica alteration assemblage accompanied by disseminated pyrite$\pm$ sphalerite occurrences associated with patchy smectite peripheral to the center of mineralization; and (6) deposition of late chalcopyrite and(or) anhydrite veinlets cutting the massive pods, followed by later veins and veinlets of barren calcite and quartz. However, the relative timing of the formation of the quartz-white mica

alteration assemblage is poorly known and possibly could have formed anytime during events "1" through "3". The intense argillic overprinting has obscured most of the textural relationships in this area. In addition, events "4" and "5" could conceivably be reversed or have occurred simultaneously.

Kuroko-type volcanogenic massive sulfide deposits have recently been described by several authors (Hogdson and Lydon, 1977; Ohmoto, 1978; Koide and Kouda, 1978; and Sillitoe, 1980) as being intimately associated with submarine calderas that have formed in a tensional back-arc tectonic environment. The regional imposition of an extensional tectonic regime would favor the emplacement of large magma chambers and failure of their roofs, thereby assisting caldera collapse. The enhanced permeability resulting from caldera-induced ring and radial fractures provides the hydrothermal fluids access to the sea floor and results in the deposition of Kuroko-type massive sulfide deposits. They represent fossil geothermal systems whose discharge points are represented by ore deposits (Hodgson and Lydon, 1977; and Henley and Thornley, 1979), particularly the stockwork ores.

Henley and Thornley (1979) have proposed a model for the genesis of Kuroko-type deposits that consists of a two-phase submarine geothermal system. Geothermal activity is established following caldera collapse or cauldron subsidence. The initial phase is a low-discharge convective

system driven by heat supplied from a postulated underlying batholith. The high silica content and glassy nature of the silicic volcanic country rocks renders them susceptible to rapid alteration and self-sealing which thereby forms an impermeable capping to the low-discharge phase. The second phase is a short-lived high-powered submarine geothermal system. This high-powered discharge results from the sudden rupture of the capping by fractures induced by seismic or gas-pressure. The polymetallic massive sulfide ore is deposited during this second phase. The source of metals is of extreme importance to this model. Henley and Thornley (1979) derive the majority of the base metals from magmatic fluids released during crystallization of plutons at depth. Some base metals may be leached from the country rocks, but this local source is considered to be subordinate. The metals are transferred to the upper part of the hydrothermal system through a buoyant vapor plume originating from the interaction of magmatic fluid and the sea water-derived geothermal fluid. During the high-powered discharge phase, the mixed fluid in the plume ascents directly to the discharge point where sulfide deposition takes place. Mineralization ends with cessation of the high-powered discharge. This termination of mineralization corresponds to the collapse of the vapor plume and the cessation of magmatism. Residual heat conducted from the shallow batholith is relatively minor and returns the high-discharge system to its former state of

low-discharge convection that may continue for several thousand years.

A modified version of the Henley and Thornley (1979) model best explains the sequence and timing of events that took place during the hydrothermal mineralization in the Seaman Gulch area (Fig. 23). The emplacement of an inferred large magma chamber served as a heat engine driving convective circulation of sea water through the volcanic pile. Minerals such as calcite and clays of the outer prpylitic zone were previously cited (see chapter on Metamorphism) as evidence that a low-discharge convective geothermal system was operative. Urabe and Sato (1978) have indicated that the products of hydrothermal alteration associated with a low-discharge system mineralogically overlap those assemblages produced during diagenesis. However, the outer propylitic zone was previously interpreted as the product of hydrothermal alteration. The early formation of chlorite and quartz (silicification) at depth in the hydrothermal system (below the discharge site of this early convective geothermal system) prior to sulfide deposition has been noted by Large (1977) as the initial stage of wall-rock alteration in volcanogenic massive sulfide deposits. Magnesium ions derived from sea water are fixed in the silicic volcanic rocks as Mg-chlorite (Large, 1977; Roberts and Reardon, 1978). Such Mg-metasomatism was noted in the discussion on chloritized silicic pyroclastic rocks from the Seaman Gulch

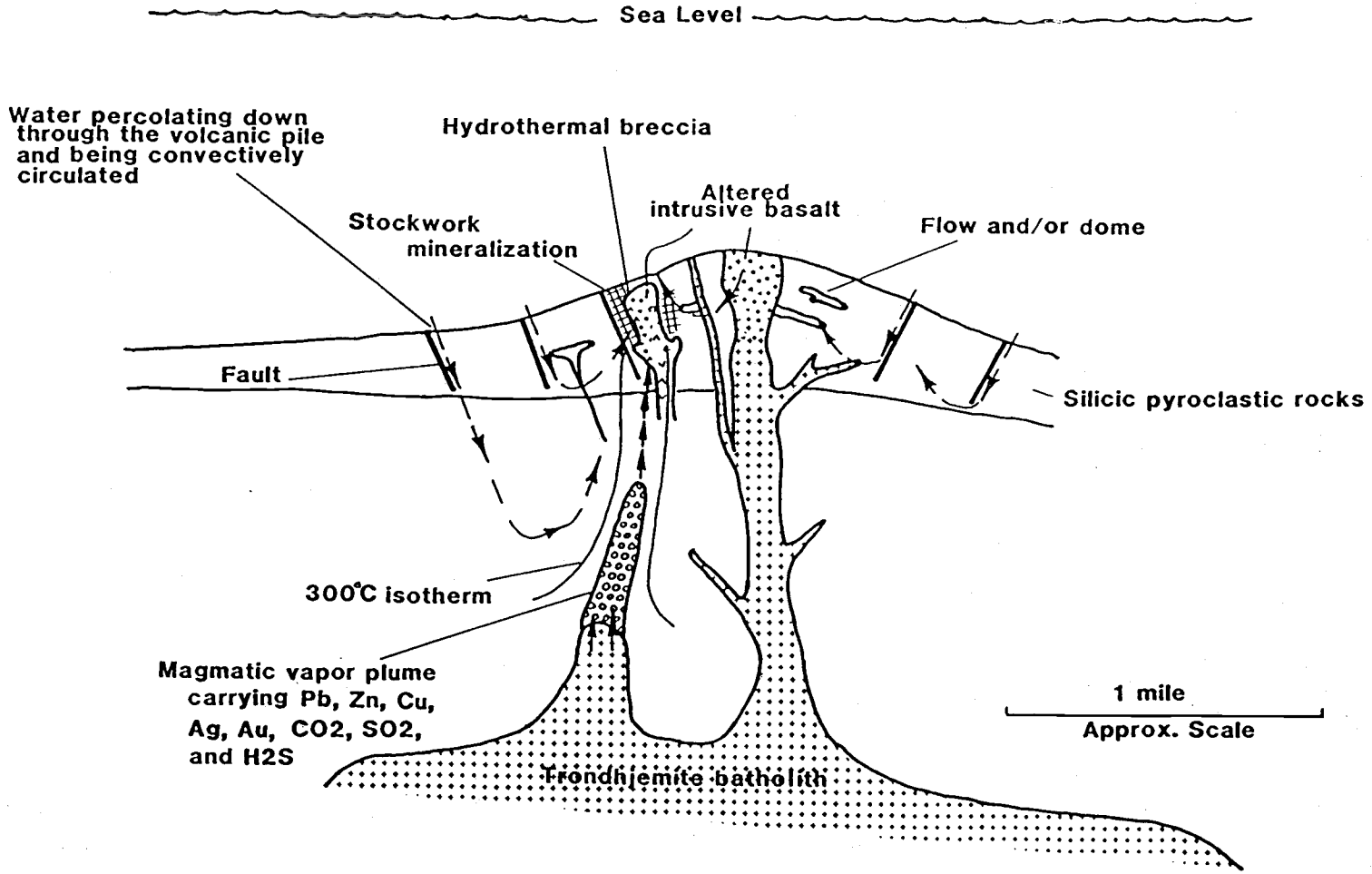

Figure 23. Schematic diagram illustrating the formation of volcanogenic stockwork-type mineralization in the Seaman Gulch area. Modified from Henley and Thornley (1979).

area. Izawa and others (1978) have concluded that MgO-enrichment is a unique feature of alteration related to Kuroko-type mineralization evolved from a sea water-dominated hydrothermal system. Evidence that a short-lived and high-powered discharge was operative in the Seaman Gulch area is found in the intimate temporal and spatial relationship between the formation of the altered basalt breccia and sulfide deposition in the adjacent silicic pyroclastic rocks. Short-term high-powered discharge may be induced by sudden rupture of the impervious roof of the system through seismic or hydraulic fracturing induced by local fluid pressure. Such a sudden event may cause hot water to flash to steam and with the consequent explosive activity forming a breccia of the host rocks. Henley and Thornley (1979) have noted that high-powered discharge to the sea floor commonly takes place through breccia pipes and vents generated by hydrothermal explosions. The high-powered discharge and related mineralization continue until wall-rock alteration and deposition of silica or calcite seal the breccia or stockwork. Breccia formation in the Seaman Gulch area took place in response to the explosive expansion of gases. Calcite localized in fracture and vugs (perhaps as a sealing agent) indicates a high CO_2 mole fraction (X_{CO_2}) in the discharge fluid (Ellis and Mahon, 1977; Burnham, 1979; Henley and Thornley, 1979; Holland and Malinin, 1979). If the deep fluid of a hydrothermal system contains more than five weight percent of dissolved

CO_2, exsolution of gasses in the upper part of the system may transmit the higher pressures that prevail at depth to the surface. Instant rupture of the country rocks may occur when the gas pressures exceed the confining pressure and the tensile strength of the rock (Henley and Thornley, 1979). Fractures may be propagated at sonic velocities toward the surface zone and then followed by a substained high-powered discharge. The inferred high-powered discharge in the Seaman Gulch area was metalliferous and precipitated sulfides. Hydrothermal deposition ceased when channelways became sealed with calcite in the altered basalt breccia and silica-sulfide±sulfate±calcite in the adjacent silicic pyroclastic rocks. Deposition of this assemblage in the silicic volcanic rocks adjacent to the altered basalt breccia that is cemented by calcite is interpreted to reflect differences in the reactivity of the two contrasting lithologies to the hydrothermal fluids. According to this model, upon cessation of the high-powered discharge, the geothermal system reverts to a low-discharge system. Continued low-discharge activity maintains a heat flow anomaly that may be reflected by the imprint of lower temperature alteration assemblages on the system in response to the encorachment of cooler fluids of the convecting seawater-dominated system (Henley and Thornley, 1979). Mineralization during this late-stage activity may include the late quartz-pyrite veinlets and some disseminations of pyrite±sphalerite associated with patchy

argillic alteration in silicic volcanic rocks found peripheral to the center of deposition.

If it is assumed that the metals contained in the hydrothermal fluids were dissolved chiefly as chloride complexes, either a decrease in temperature or a general increase in pH would be the most effective causes of the precipitation of the sulfide and gangue minerals (Helgeson, 1969; Urabe and Sato, 1978; Skinner, 1979; Burnham, 1979; Henley and Thornley, 1979). A decrease in temperature can be accomplished by mixing the ascending ore fluids with cooler sea water. Boiling that occurs concurrently during explosive breccia formation generally produces an increase in pH as well as the exsolution of gases (Urabe and Sato, 1978). The vertical zonation of metals found in the Seaman Gulch area may be explained by differential precipitation from a cooling polymetallic hydrothermal solution as it ascended through the host rocks. This explanation for the vertical zoning of metals is analogous to that proposed by Sato (1977) for the Kuroko-type massive sulfide deposits. Moreover, such preferential transportation and precipitation of base metals in response to diminishing (decreasing) temperatures and increasing pH has also been postulated by Large (1977).

Implications that boiling played a critical role in the precipitation of sulfide and gangue minerals is significant. Should boiling occur below the sea floor-sea water interface, as noted by Sato (1977), ore deposition

should not take place on the sea floor. Such a regime might be illustrated by a deposit that is characterized by well-developed stockwork ore but exhibits only traces of stratiform massive ore. This is the case for the Seaman Gulch area, where stockwork-type epigenetic mineralization is present, but an overlying syngenetic massive sulfide body is noticeably absent. However, there are several alternative explanations to account for the absence of a stratiform massive body overlying the stockwork mineralization. These might include such mechanisms as (1) mechanical transportation away from the vent area via local slumping or incorporation in large debris flows (olistostromes) as suggested by Eastoe and others (1987); (2) precipitation of distal-type massive sulfide deposits away from the vent area; (3) structural displacement or dismemberment; (4) subsequent erosion; or (5) combinations thereof.

The role of boiling was presumably significant in the precipitation of calcite, and less so for anhydrite. Boiling may lead to the deposition of virtually all minerals, but it is probably most significant for the carbonates, particularly calcite, according to Holland and Malinin (1979). Calcite and anhydrite are found as coexisting gangue minerals interstital to the sulfides in some of the massive pod occurrences; particularly those adjacent to the altered intrusive basalt. Boiling and an increase in the solution pH may move the hydrothermal fluid toward

saturation with respect to anhydrite, but the effect is much less pronounced than for calcite (Holland, and Malinin, 1979). If sea water is heated in excess of 110°C anhydrite will begin to precipitate, especially in the presence of basalt (Holland and Malinin, 1979). The location of the coexisting assemblages of calcite and anhydrite in and proximal to the altered intrusive basalt suggest that the chief source of CaO was the basalt. Lime (CaO) was released during reactions between hydrothermal fluids and basalt prior to or concurrently with the exsolution of CO_2 during boiling, which thereby caused precipitation of calcite. Heating of sea water accompanied by interaction with country rocks, or mixing of ascending hydrothermal solutions with sea water at a site above or below the sea water-sediment interface are the mechanisms favored by Farrel and others (1978), Shikazono (1983), and Kusakabe and Chiba (1983) to explain the deposition of anhydrite from the Kuroko deposits. These studies have focused on the stratiform anhydrite-gypsum (Sekkoko) occurrences.

The zone of mixing between the ascending metalliferous hydrothermal fluids and sea water may be marked by the transition between the zones of chlorite and quartz-white mica alteration. This transitional zone is characterized by the appearance of anhydrite in coexistence with some of the polymetallic sulfides. The precipitation of anhydrite is considered significant because it is possibly the result

of an increase in the activity of the sulfate ion if conditions were such that the activity of CaO and temperature are relatively constant. Increase in the activity of the sulfate ion may be caused either by the oxidation of H_2S or by the incorporation of sea water (Urabe and Sato, 1978). These authors favor the latter mechanism. The sea water sulfate incorporated into a chemically reduced hydrothermal fluid may persist "metastably" due to slow rates of reaction associated with processes of inorganic reduction (Urabe and Sato, 1978). As the hydrothermal fluid becomes less reduced upon increased mixing with sea water, it is possible that the sulfide-forming environment is preserved with H_2S remaining the dominant sulfur species (relatively small amounts of anhydrite coexisting with late pyrite and chalcopyrite) and with the chemical environment at or near the sulfide-sulfate equilibrium boundary (coexisting sulfides and fulates). The favored mechanism for controlling the increased oxygen fugacity is the following reaction,

$$Fe^{2+} + 2H_2S + 1/2\ O_2 \rightleftarrows FeS_2 + 2H^+ + H_2O \qquad (1)$$

in which H_2S (or HS^-) is the dominant aqueous sulfur species of the hydrothermal fluid according to Urabe and Sato (1978). Therefore, providing sufficient iron is contained in solution, this reaction can consume the maximum amount of oxygen contained in sea water (Urabe and Sato, 1978). This hypothetical model may account for the

presence of the coexisting sulfide-sulfate assemblage found in the transitional zone. Alterantively, or concurrently, with the precipitation of pyrite as suggested in equation (1), the precipitation of anhydrite will deplete the hydrothermal fluid of sulfate ions. With deposition of sulfate, the oxygen fugacity is proportionately decreased, thus favoring deposition of sulfides (Helgeson, 1979).

In contrast, the model of Henley and Thornley, as previously noted, requires a crucial magmatic contribution. This model is favored over circulating sea water models requiring the wholesale leaching of base metals from the country rocks during the convection of hydrothermal fluids (e.g. Ohmoto and Rye, 1974; Franklin, 1986). Models that require the leaching of base metals are based primarily on evidence provided by stable isotopes, which indicate for the type-section Kuroko deposits of Japan that sea water was the major source of water and sulfur in the ore-forming hydrothermal fluid. Although the isotopic evidence is impressive, most of these data are based on samples from the stratiform massive ore that precipitated at the sea floor - sea water interface. According to Henley and Thornley (1979), the chemical and isotopic signatures inherited from the deeper-seated magmatic vapor plume are progressively diluted as a consequence of near-surface mixing with the sea water dominated hydrothermal fluid. Significant dilution is to be expected by the time the fluid plume ascends to the vicinity of the stockwork zone

and (or) vents on the sea floor. Fluid inclusion studies by Urabe and Sato (1978) have demonstrated that salinities are generally greater than normal sea water. Moreover, fluid inclusions of the stockwork zone are normally more saline than those of the overlying Kuroko-zone (massive sulfide body). The less saline fluid inclusions were probably diluted as a result of mixing with sea water. Thus, proportions of the more saline magmatic waters in the hydrothermal fluids are likely to have been much larger prior to discharge onto the sea floor. The downward increase in the salinities of fluid inclusions does not prove a magmatic contribution from depth as similar increases can be produced by boiling. However, boiling has not been documented from the type-area for Kuroko deposits. Because current isotopic techniques cannot distinguish magmatic contributions of less than 10 percent, possible magmatic signatures in the final ore-forming hydrothermal fluid may be difficult to identify. Moreover, the isotopic characteristics that might be indicative of a magmatic source would be progressively obliterated by dissolution and mineral fluid reactions characterized by isotopic exchange during the late-stage low-discharge geothermal activity. Thus, evidence of the original magmatic source may be only locally preserved and probably at depth well below the zone of economic mineralization. On the basis of studies in the Creede District, Colorado, Wetlaufer and others (1979) have suggested that active geothermal systems

that now have only one isotopically identifiable source of water may have been dominated by different waters in the past, and that they may be enveloped by yet different waters in the future. The stable isotope data that imply sea water as the major hydrous component of the hydrothermal fluid are not likely to be refuted. However, it is possible that such fluids became sufficiently abundant in the near surface (sea floor) environment to the point of masking a magmatic contribution that was present at depth. Nonetheless, these sea water-dominated fluids might continue to serve as an important metal transporting agent. Overemphasis of stable isotope data that indicates the predominance of sea water during the formation of volcanogenic massive sulfide deposits may be misleading with respect to the provenance or source of both the fluids and the metals. Similar caution has been advocated by Sawkins and Scherkenbach (1981) for the origin of base metals in the breccia pipes at Cananea, Mexico. In addition, investigators such as Ishihara and Terashima (1974), Sato (1977), Urabe and Sato (1978), Ishihara and Sasaki (1978), Bryndzia and others (1983), and Williams (1986) have cited evidence (including isotopes) to support a magmatic contribution to the sea water-dominated fluids that have formed volcanogenic massive deposits.

Economic Potential

The economic potential of the Seaman Gulch area is

considered to be low. Sulfide minerals occur chiefly as disseminations and stringer veinlets. The grades and spatial distribution of the sulfide occurrences, in general, do not favor the development of economically attractive mineralization in terms of tonnage and grade.

The chief indicators of sulfide mineralization in the Seaman Gulch area are the presence of sulfide minerals and their oxidized equivalents (gossan), hypogene and supergene wall rock alteration that is spatially associated with the sulfide mineralization, and large sulfide-bearing fissure quartz veins in close proximity to the mineralized areas. Two other areas in the vicinity of Seaman Gulch exhibit these characteristics. They are: (1) the NW¼, SE¼, Sec. 16; and (2) the SW¼, SW¼, Sec. 9. Examination of these two mineralized areas disclosed that they lack identifiable base metal-bearing sulfides. Moreover, the exposed mineralization extends over a much smaller surface area than that centered in the NE¼, Sec. 17 and NW¼, Sec. 16. Hence, they are considered to be economically unimportant.

GEOLOGIC SUMMARY

The geologic record at the Seaman Gulch area began during the Upper Permian when submarine volcanism was initiated in an oceanic (?) island arc tectonic setting, westward of the western margin of the Cordillera. Mafic flows and pyroclastic rocks of the Upper Permian Dekkas Andesite accumulated within the arc proper and are the oldest rocks exposed in this area. Silicic volcanism followed during Late Permian times. Rapid eruption and deposition of the silicic volcanics that comprise the Bully Hill Rhyolite took place. Minor amounts of mafic (altered basalt) rock were subsequently intruded into the silicic volcanic pile. Faults and fractures provided increased permeability to sea water that was heated and convectively circulated. It is suggested that fluids were released from magmas at depth and were entrained in the convecting hydrothermal cells, adding heat, volatiles, and base and precious metals to these hydrothermal systems. The metals were discharged at submarine hot springs onto the sea floor where, in the East Shasta District, they precipitated to form the stratiform massive sulfide deposits. The massive sulfide deposits in the East Shasta District consist of two types of ore, massive sulfides and stringers. The massive sulfides are conformable with the stratigraphy (i.e. syngenetic), but the stringer ore clearly cuts the stratigraphy underlying the massive sulfide lenses (i.e.

epigenetic). However, in the Seaman Gulch area, sulfides including pyrite, sphalerite, chalcopyrite, tetrahedrite-tennantite, and galena are present chiefly as disseminations, stringer veinlets, and massive pods. Thus, only the epigenetic stringer-type sulfide occurrences were deposited in the area. Distribution of the sulfides displays a crude zonation and from bottom to top is as follows; pyrite-chalcopyrite as disseminations and stringer veinlets, pyrite-chalcopyrite-sphalerite as disseminations, stringer veinlets, and networks, and pyrite-chalcopyrite-sphalerite-tetrahedrite-tennantite-galena as disseminations, stringer veinlets, and massive pods. Controls that served to localize the occurrences of sulfides are intrusive rock-country rock contacts and the permeability and porosity of pyroclastic rocks, faults, and fractures. Alteration assemblages produced during movement of hydrothermal fluids through the volcanic pile include chloritic alteration, quartz-white mica alteration, propylitic alteration, silicification, argillic alteration, and carbonate alteration. These alteration assemblages display both vertical and lateral zonations. A central zone of chloritic alteration grades laterally into propylitic alteration and upward into quartz-white mica alteration. The quartz-white mica alteration in turn grades laterally into propylitic alteration. Argillic alteration and carbonate alteration are genetically related but slightly later events that overprint the earlier assemblages. Concurrent

with this hydrothermal activity, clastic sedimentation began and shale of the Pit Formation was deposited along with interbeds of silicic pyroclastic rocks during the waning stages of volcanism. These rocks underwent deformation during Middle (?) or Late Jurassic time, although secondary mineral assemblages found in the Seaman Gulch area do not indicate a significant regional metamorphic overprint on the previously described widespread hydrothermal event. The Seaman Gulch area was later uplifted and eroded until the Pliocene time, and subsequently was buried by lahars that originated from Cascade volcanoes to the east. Thereafter, erosion resumed but was interspersed with episodic eruptions of pyroxene andesite or basalt to fill topographic lows during Pliocene and Pleistocene-Recent time. Mineral deposits of the Seaman Gulch area are considered to be of negligible economic importance because of their small size, low grade, and absence of stratiform massive sulfide accumulations.

BIBLIOGRAPHY

Albers, J.P., 1953, Geology and ore deposits of the Afterthought Mine, Shasta County, California: Calif. Div. Mines Spec. Rept. 29, 18p.

_____, 1959, Soda metasomatism in the East Shasta copper-zinc district, northern California: Geol. Soc. India, v. 1, p. 31-43.

_____, 1966, Economic deposits of the Klamath Mountains: Calif. Div. Mines and Geology Bull. 190, p. 51-64.

Albers, J.P. and Robertson, J.F., 1961, Geology and ore deposits of the East Shasta copper-zinc district, Shasta County, California: U.S. Geol. Survey Prof. Paper 338, 107 p.

Albers, J.P., Kistler, R.W., and Kwak, Loretta, 1981, The Mule Mountain Stock, an early Middle Devonian pluton in northern California; Isochron West, v. 31, p. 17.

Albers, J.P. and Bain, J.H.C., 1985, Regional setting and new information on some critical geologic features of the West Shasta District, California: Econ. Geology, v. 80, p. 2072-291.

Anderson, C.A., 1983, The Tuscan Formation of northern California, with a discussion concerning the origin of volcanic breccias: Univ. Calif. Pubs. Geol. Sciences Bull., v. 23, 56p.

_____, 1969, Massive sulfide deposits and volcanism: Econ. Geology, v. 64, p. 129-146.

Barker, Fred, Millard, M.T., and Knight, R.J., 1979, Reconnaissance geochemistry of Devonian island-arc volcanic and intrusive rocks, West Shasta district, California, in Barker, Fred, ed., Trondhjemites, dacites and related rocks: Amsterdam, Elsevier, p. 401-414.

Bence, A.E. and Taylor, B.E., 1985, Rare earth element systematics of West Shasta metavolcanic rocks: Petrogenesis and hydrothermal alteration: Econ. Geology, v. 80, p. 2164-2176.

Blanchard, Roland, 1968, Interpretation of leached outcrops: Nev. Bur. Mines Geology Bull. 66, 198 p.

Bond, G.C., 1973, A late Paleozoic volcanic arc in the eastern Alaska Range, Alaska: Jour. Geology, v. 81, p. 557-575.

Boyle, A.C., 1914, The geology and ore deposits of the Bully Hill mining district, California: Amer. Inst. Mining Eng. Trans., v. 48, p. 67-117.

Bryndzia, L.T., Scott, S.D., and Farr, J.E., 1983, Mineralogy, geochemistry, and mineral chemistry of siliceous ore and altered footwall rocks in the Uwamuki 2 and 4 deposits, Kosaka Mine, Hokuroko District, Japan: Econ. Geology Mono. 5, p. 507-522.

Burhmam, C.W., 1979, Magmas and hydrothermal fluids, in Barnes, H.L., ed., Geochemistry of the hydrothermal ore deposits, 2nd ed.: New York, John Wiley and Sons, p. 71-136.

Churkin, Michael, Jr., and Eberlien, G.D., 1977, Ancient borderland terranes of the North American Cordillera: Correlation and microplate tectonics: Geol. Soc. America Bull., v. 93, p. 1208-1231.

Colley, H., 1976, Classification and exploration guide for Kuroko-type deposits based on occurrences in Fiji: Trans. Inst. Min. Metall., Sec. B, v. 85, p. 190-199.

Colley, H. and Rice, C.M., 1975, A Kuroko-type deposit in Fiji: Econ. Geology, v. 70, p. 1373-1386.

Condie, K.C. and Snansieng, S., 1971, Petrology and geochemistry of the Duzel (Ordovician) and Gazelle (Silurian) Formations, northern California: Jour. Sed. Petrology, v. 41, p. 714-541.

Coogan, A.H., 1960, Stratigraphy and paleontology of the Permian Nosoni and Dekkas Formations (Bollibokka Group): Univ. Calif. Publ. Geol. Sci., v. 36, p. 243-316.

Creasy, S.C., 1959, Some phase relations in hydrothermally altered rocks of porphyry copper deposits: Econ. Geology, v. 54, p. 768-784.

Curtis, D.R., 1983, Stratigraphy and origin of the Pit Formation, northern California: unpubl. M.S. thesis, Univ. of California, Berkeley, 59p.

Davis, G.A., 1966, Metamorphic and granitic history of the Klamath Mountains: Calif. Div. Mines and Geology Bull. 190, p. 39-50.

Davis, G.A., Holdaway, M.J., Lipman, P.W., and Romey, W.D., 1965, Structure, emtamorphism, and plutonism in the south-central Klamath Mountains, California: Geol. Soc. America Bull., v. 76, p. 933-966.

Diller, J.S., 1893, Tertiary evolution of the topography of the Pacific Coast: U.S. Geol. Survey, 14th Ann. Rept., pl. 45, p. 414.

_____, 1903a, Klamath Mountain section, California: Amer. Jour. Science, 4th series, v. 165, p. 342-362.

_____, 1903b, Copper deposits of the Redding region, California: U.S. Geol. Survey Bull. 213, p. 123-132.

_____, 1906, Description of th Redding quadrangle (California): U.S. Geol. Survey Geol. Atlas Folio 138, 14p.

Doe, B.R. and Zartman, R.E., 1979, Plumbotectonics, the Phanerozoic, in Barnes, H.L., ed., Geochemistry of the hydrothermal ore deposits: New York, John Wiley and Sons, p. 22-70.

Eastoe, C.J., Gustin, M.M., and Nelson, S.E., 1987, Problems of recognition of olistostromes: An example from the lower Pit Formation, eastern Klamath Mountains, California: Geology, v. 15, p. 541-544.

Ellis, A.J. and Mahon, W.A.J., 1977, Chemistry and geothermal systems: New York, Academic Press, 392 p.

Everndon, J.F., Savage, D.E., Curtis, G.H. and James, G.T., 1964, Potassium argon dates and the Cenozoic mammalian chronology of North America: Amer. Jour. Science, v. 262, p. 145-198.

Ewart, A., Bryan, W.B., and Gill, J.B., 1973, Mineralogy and geochemistry of the younger volcanic islands of Tonga, Southwest Pacific: Jour. Petrology, va. 14, p. 429-465.

Fahan, M.R. and Wright, J.E., 1983, Plutonism, volcanism, folding, regional metamorphism and thrust faulting: contemporarneous aspects of a major Middle Jurassic orogenic event within the Klamath Mountains, California: Geol. Soc. America Abstr. with Programs, v. 15, no. 5, p. 272-273.

Fairbanks, H.W., 1893, Geology and mineralogy of Shasta County, California: Calif. Mining Report 11, p. 24-53.

Farrell, C.W., Holland, H.D., and Peterson, Ulrich, 1978, The isotopic composition of strontium in barites and anhydrites from Kuroko deposits: Mining Geology, v. 28, p. 281-291.

Fisher, R.V., 1961, Proposed classification of volcaniclastic sediments and rocks: Geol. Soc. America Bull., v. 72, p. 1409-1414.

_____, 1966, Rocks composed of volcanic fragments: Earth Sci. Reviews, v. 1, p. 287-298.

Fisher, R.V. and Schmincke, H.-U., 1984, Pyroclastic Rocks: Berlin, Springer-Verlag, 472 p.

Fiske, R.S., 1963, Subaqueous pyroclastic flows in the Ohanapecosh Formation, Washington: Geol. Soc. America Bull., v. 74, p. 391-406.

Fiske, R.S. and Matsuda, T., 1964, Submarine equivalents of ash flow tuffs in the Tokiwa Formation, Japan: Amer. Jour. Science, v. 262, p. 76-106.

Franklin, J.W., 1986, Volcanic-associated massive sulfide deposits - an update, in Andrew, C.J., Crowe, R.W.A., Finlay, S., Pennel, W.M., and Pyne, J.F., eds., Geology and genesis of mineral deposits in Ireland: Irish Assoc. for Econ. Geology, p. 49-70.

Fraticelli, L.A., 1984, Geology of portions of the Project City and Bella Vista quadrangles, Shasta County, California: unpubl. M.S. thesis, California State Univ., San Jose, 110 p.

Fredericks, P.E., 1980, Volcanic lithofacies and massive sulfide mineralization, East Shasta District, California: unpubl. M.S. thesis, Univ. of Texas, Austin, 110 p.

Furnes, H., Fridleifsson, I.B., and Atkins, F.B., 1980, Subglacial volcanics - on the formation of acid hyaloclastics: Jour. Volc. and Geoth. Research, v. 8, p. 95-110.

Graton, L.C., 1909, The occurrence of copper in Shasta County, California: U.S. Geol. Survey Bull. 430-B, p. 71-111.

Griscom, A., 1977, Aeromagnetic and gravity interpretation of the Trinity ophiolite complex, northern California: Geol. Soc. America Abstracts with Programs, v. 9, p. 426-427.

Gustin, M.M. and Eastoe, C.J., 1986, Geology and mineralization of the Bully Hill area, East Shasta District, California: Geol. Soc. America Abstracts with Programs, v. 18, no. 2, p. 103.

Helgeson, H.C., 1969, Thermodynamics of hydrothermal systems at elevated temperatures and pressures: Amer. Jour. Science, v. 267, p. 729-804.

_____, 1979, Mass transfer among minerals and hydrothermal solutions, in Barnes, H.L., ed., Geochemistry of the hydrothermal ore deposits: New York, John Wiley and Sons, p. 568-610.

Henley, R.W. and Thornley, R., 1979, Some geothermal aspects of polymetallic massive sulfide formation: Econ. Geology, v. 74, p. 1600-1612.

Hilton, R.P., 1975, The geology of the Ingot-Round Mountain area, Shasta County, Califonria: unpubl. M.A. thesis, California, Chico, 83 p.

Hinds, N.E.A., 1932, Paleozoic eruptive rocks of the southern Klamath Mountains: Calif. Univ. Publ. Geol. Sci. Bull., v. 20,p. 375-410.

_____, 1935, Mesozoic and Cenozoic eruptive rocks of the southern Klamath Mountains, California: Calif. Univ. Publ. Geol. Sci. Bull., v. 23, p. 313-380.

_____, 1940, Paleozoic section in the southern Klamath Mountains, California, in Pacific Sci. Cong., 6th, Berkeley, Calif., 1940 Proc.: Calif. Univ. Press, v. 1, p. 273-287.

Hodgson, C.J. and Lydon, J.W., 1977, Geologic setting of volcanogenic massive sulfide deposits and active hydrothermal systems: some implications for exploration: Canad. Min. Metall. Bull., v. 70, p. 360-366.

Holland, H.D. and Malinin, S.D., 1979, The solubility and occurrence of non-ore minerals, in Barnes, H.L., ed., Geochemistry of the hydrothermal ore deposits, 2nd ed.: New York, John Wiley and Sons, p. 461-508.

Hopson, C.A. and Mattinson, J.M., 1973, Ordovician and Late Jurassic ophiolite assemblages in the Pacific Northwest: Geol. Soc. America Programs with Abst., v. 5, no. 1, p. 57.

Hotz, P.E., 1971, Plutonic rocks of the Klamath Mountains, California and Oregon: U.S. Geol. Survey Prof. Paper 684-B, p. B1-B20.

_____, 1974, Preliminary geologic map of the Yreka Quadrangle, California: U.S. Geol. Survey MF-568.

_____, 1977, Geology of the Yreka Quadrangle, Siskyou County, California: U.S. Geol. Survey Bull. 1436, 72 p.

Hutchinson, R.W., 1973, Volcanogenic massive sulfide deposits and their metallogenic significance: Econ. Geology, v. 68, p. 1223-1246.

Irwin, W.P., 1960, Geologic reconnaissance of the northern Coast Ranges and Klamath Mountains, California, with a summary of mineral resources: Calif. Div. Mines and Geology Bull. 179, 80 p.

Irwin, W.P., 1966, Geology of the Klamath Mountains Province: Calif. Div. Mines and Geology Bull. 190, p. 17-37.

Irwin, W.P. and Bath, G.P., 1962, Magnetic anomalies and ultramafic rock in northern California: U.S. Geol. Survey Prof. Paper 450-B, p. 65-67.

Irwin, W.P. and Lipman, P.W., 1962, A regional ultramafic sheet in eastern Klamath Mountains, California: U.S. Geol. Survey Prof. Paper 450-C, p. 18-21.

Ishihara, Shunsho and Sasaki, A., 1978, Sulfur of Kuroko deposits - a deep seated origin?: Mining Geology, v. 28, p. 361-367.

Ishihara, Shunsho and Terashima, Shigeru, 1974, Base metal contents of the basement rocks of Kuroko deposits, in Ishihara, Shunsho, ed., Geology of Kuroko deposits: Mining Geology Spec. Issue No. 6, p. 421-428.

Izawa, Eiji, Yoshido, Tetsuo, and Saito, Ryo, 1978, Geochemical characteristics of hydrothermal alteration around Fukazawa Kuroko deposit, Akita, Japan: Mining Geology, v. 28, p. 325-335.

Jakes, P. and White, A.J.R., 1972, Major and trace element abundances in volcanic rocks of orogenic areas: Geol. Soc. America Bull., v. 83, p. 29-40.

Kinkel, A.R., Jr., Hall, W.E. and Albers, J.P., 1956, Geology and base-metal deposits of West Shasta copper-zinc district, Shasta County, California: U.S. Geol. Survey Prof. Paper 285, 156 p.

Kistler, R.W., McKee, E.H., Futa, K., Peterman, Z.E., and Zartman, R.E., 1985, A reconnaissance Rb-Sr, Sm-Nd, U-Pb, and K-Ar study of some host rocks and ore minerals in the West Shasta Cu-Zn District, California: Econ. Geology, v. 80, p. 2128-2135.

Koide, Hitoshi and Kouda, Ryoichi, 1978, Ring structures, resurgent cauldron, and ore deposits in the Hokuroko volcanic field, northern Akita, Japan: Mining Geology, v. 28, p. 233-244.

Kusakabe, Minoru and Chiba, Hitoshi, 1983, Oxygen and sulfur isotope composition of barite and anhydrite from the Fukazawa Deposit, Japan; Econ. Geology Mono 5, p. 292-301.

LaFehr, T.R., 1966, Gravity in the eastern Klamath Mountains, California: Geol. Sco. America Bull., v. 77, p. 1177-1190.

Lanphere, M.A., Irwin, W.P., and Hotz, P.E., 1968, Isotopic age of the Nevadan orogeny and older plutonic and metamorphis events in the Klamath Mountains, California: Geol. Soc. America Bull, v. 79, p. 1027-1052.

Lapierre, H., Cabanis, B., Coulon, C., Brouxel, M., and Albarede, F., 1985, Geodynamic setting of Early Devonian Kuroko-type sulfide deposits in the eastern Klamath Mountains (northern California) inferred by the petrological and geochemical characteristics of the associated island-arc volcanic rocks: Econ. Geology, v. 80, p. 2100-2113.

Large, R.R., 1977, Chemical evolution and zonation of massive sulfide deposits in volcanic terrains: Econ. Geology, v. 72, p. 549-572.

LeMaitre, R.W., 1976, The chemical variability of some common igneous rocks: Jour. Petrology, v. 17, p. 589-637.

Lindsley-Griffin, Nancy, 1977, The Trinity ophiolite, Klamath Mountains, California, in Coleman, R.G. and Irwin, W.P., eds., North American ophiolites: Oregon Dept. Geology Mineral Industr. Bull. 95, p. 107-120.

Lydon, P.A., 1969, Geology and lahars of the Tuscan Formation, northern California, in Coats, R.R., Hay, R.L., and Anderson, C.A., eds., Studies in volcanology: Geol. Soc. America Memr. 116, p. 441-476.

Mattinson, J.M. and Hopson, C.A., 1972, Paleozoic ages of rocks from ophiolitic complexes in Washington and northern California: Trans. Amer. Geophys. Union, v. 53, p. 543.

McBirney, A.R., 1969, Compositional variations of Cenozoic calc-alkaline suites of Central America, in McBirney, A.R., ed., Proceedings of the Andesite conference: Oregon Dept. Geology Mineral Industr. Bull. 65, p. 185-190.

Miller, M.M., 1986, Tectonic evolution of late Paleozoic island-arc sequences in the western U.S. Cordillera; with detailed studies from the eastern Klamath Mountains, northern California: unpubl. Ph.D. thesis, Stanford University, Stanford, California, 201 p.

Miller, M.M. and Wright, J.E., 1987, Paleogeographic implications of Permian Tethyan corals from the Klamath Mountains, California: Geology, v. 15, p. 266-269.

Murray, M. and Condie, K.C., 1973, Post-Ordovician to early Mesozoic history of the eastern Klamath subprovince, northern California: Jour. Sed. Petrology, v. 43, p. 505-515.

Nelson, S.E., 1986, The geology and mineralization potential of the Bella Vista-Ingot area, Shasta County, California: unpubl. M.S. thesis, Univ. of Arizona, Tucson, 121 p.

Ohmoto, Hiroshi, 1978, Submarine calderas: a key to the formation of volcanogenic massive sulfide deposits: Mining Geology, v. 28, p. 219-231.

Ohmoto, Hiroshi and Rye, R.O., 1974, Hydrogen and oxygen isotopic compositions of fluid inclusions in the Kuroko deposits, Japan: Econ. Geology, v. 69, p. 947-953.

Palache, Charles, Berman, Harry, and Frondel, Clifford, 1944, Dana's system of mineralogy, Vol. 1, 7th ed.: New York, John Wiley and Sons, 834 p.

Potter, A.W., Hotz, P.E., and Rohr, D.M., 1977, Stratigraphy and inferred tectonic framework of Lower Paleozoic rocks in the eastern Klamath Mountains, northern California, in Stewart, J.H., Stevens, C.H., and Fritsche, A.E., eds., Paleozoic paleogeography of the western United States: Pacific Section Soc. Econ. Paleont. Mineral., p. 421-440.

Ribbe, P.H., 1975, Optical properties and lattice parameters of plagioclase feldspars, in Ribbe, P.H., ed., Feldspar mineralogy: Mineral. Soc. America Short Course Notes, v. 2, p. R-53-R-72.

Roberts, R.G. and Reardon, E.J., 1978, Alteration and ore-forming process at Mattagami Lake Mine, Quebec: Canad. Jour. Earth Sci., v. 15, p. 1-21.

Russell, R.D. and VanderHoff, V.L., 1931, A vertebrate fauna from a new Pliocene formation in northern California: Calif. Univ. Dept. Geol. Sci. Bull., v. 20, no. 2, p. 11-21.

Sato, Takeo, 1977, Kuroko deposits, their geology, geochemistry and origin, in Volcanic processes and ore genesis: Geol. Soc. London Spec. Publ. 7, p. 153-161.

Sawkins, F.J., 1976, Massive sulfide deposits in relation to geotectonics, in Strong, D.F., ed., Metallogeny and plate tectonics: Geol. Assoc. Canada Spec. Publ. 14, p. 221-240.

Sawkins, F.J. and Scherkenbach, D., 1981, High copper contents of fluid inclusions in quartz from northern Sonora: implications for ore genesis theory: Geology, v. 9, p. 37-40.

Schermerhorn, L.J.G., 1973, What is a keratophyre?: Lithos, v. 6, p. 1-11.

Shikazono, Naotatsu, Holland, H.D., and Quirk, R.F., 1983, Anhydrite in Kuroko deposits: mode of occurrence and depositional mechanisms: Econ. Geology Mono. 5, p. 329-344.

Silberling, N.J. and Jones, D.L., 1982, Tectonic significance of Permian-Triassic strata in northwestern Nevada and northern California: Geol. Soc. America Abstracts with Programs, v. 14, no. 4, p. 234.

Sillitoe, R.H., 1980, Are porphyry copper and Kuroko-type massive sulfide deposits incompatible?: Geology, v. 8, p. 11-14.

Skinner, B.J., 1979, The many origins of hydrothermal mineral deposits, in Barnes, H.L., ed., Geochemistry of the hydrothermal ore deposits, 2nd ed.: New York, John Wiley and Sons, p. 1-21.

Skinner, J.W. and Wilde, G.L., 1965, Permian biostratigraphy and fusulinid faunas of the Shasta Lake area, northern California, in proterozoa, Article 6: Univ. of Kansas Paleont. Contrib., H.N. Fiske Mem. Papers, 90 p.

Stevens, C.H., Miller, M.M., and Nestell, Merlynd, 1987, A new Permian waagenophyllid coral from the Klamath Mountains, California: Jour. of Paaleont., v. 61, p. 690-699.

Tomblin, J.F., 1979, Dacite of the Lesser Antilles, in Barker, Fred, ed., Trondhjemites, dacites and related rocks: Amsterdam, Elsevier, p. 601-628.

Turner, F.J., 1981, Metamorphic petrology, 2nd ed.: New York, McGraw Hill, 524 p.

Urabe, Tetsuro, 1974, Mineralogical aspects of the Kuroko deposits in Japan and their implications: Mineral. Deposita, v. 8, p. 322-348.

Urabe, Tetsuro and Sato, Takeo, 1978, Kuroko deposits of the Kosaka Mine, northeast Honshu, Japan - products of submarine hot springs on Miocene sea floor: Econ. Geology, v. 73, p. 161-179.

Vallance, T.G., 1969, Spilites again: some consequences of the degradation of basalt: Linnean Soc. New South Wales Proc., v. 94, p. 8-50.

Vance, J.A., 1965, Zoning in igneous plagioclase: patchy zoning: Jour. Geology, v. 72, p. 636-651.

Watkins, Rodney and Stensrud, H.L., 1983, Age of sulfide ores in the West Shasta and East Shasta Districts, Klamath Mountains, California: Econ. Geology, v. 78, p. 340-343.

Wells, F.G., Walker, G.W., and Merriam, C.W., 1959, Upper Ordovician(?) and Upper Silurian formations of the northern Klamath Mountains, California: Geol. Soc. America Bull., v. 70, p. 645-649.

Wetlaufer, P.H., Bethke, P.M., Barton, P.R., Jr., and Rye, R.O., 1979, The Creede Ag-Pb-Zn-Cu-Au District, central San Juan Mountains, Colorado: A fossil geothermal system, in Ridge, J.D., ed., Papers on mineral deposits of western North America: Nev. Bur. Mines Geology Rept. 33, p. 159-164.

Wheeler, H.E., 1940, Permian volcanism in western North America, in Pacific Sci. Cong., 6th, Berkeley, Calif., 1940, Proc.: Calif. Univ. Press, v. 1, p. 369-376.

Williams, F.M., Sheppard, W.A. and McArdle, P., 1986, Avoca Mine, Co. Wicklow: a review of geological and isotope studies, in Andrews, C.J., Crowe, R.W.A., Finlay, S., Pennell, W.M. and Pyne, J.F., eds., Geology and genesis of mineral deposits in Ireland: Irish Assoc. for Econ. Geology, p. 71-82.